

**FABRICATION OF POLY (DL-LACTIC-CO-GLYCOLIC ACID)  
NANOPARTICLES AND SYNTHETIC PEPTIDE DRUG CONJUGATE FOR  
ANTI-CANCER DRUG DELIVERY**

**A THESIS SUBMITTED TO  
THE GRADUATE SCHOOL OF NATURAL AND APPLIED SCIENCES  
OF  
MIDDLE EAST TECHNICAL UNIVERSITY**

**BY**

**GÜLSEREN PETEK ŞEN**

**IN PARTIAL FULFILLMENT OF THE REQUIREMENTS  
FOR  
THE DEGREE OF MASTER OF SCIENCE  
IN  
BIOTECHNOLOGY**

**DECEMBER 2009**

Approval of the thesis:

**FABRICATION OF POLY (DL-LACTIC-CO-GLYCOLIC ACID)  
NANOPARTICLES AND SYNTHETIC PEPTIDE DRUG CONJUGATE FOR  
ANTI-CANCER DRUG DELIVERY**

submitted by **GÜLSEREN PETEK ŞEN** in partial fulfillment of the requirements  
for the degree of **Master of Science in Biotechnology, Middle East Technical  
University** by,

Prof. Dr. Canan Özgen \_\_\_\_\_  
Dean, Graduate School of **Natural and Applied Sciences**

Prof. Dr. İnci Erođlu \_\_\_\_\_  
Head of Department, **Biotechnology**

Prof. Dr. Ufuk Gündüz \_\_\_\_\_  
Supervisor, **Biology Dept., METU**

Prof. Dr. Güngör Gündüz \_\_\_\_\_  
Co-Supervisor , **Chemical Engineering Dept., METU**

**Examining Committee Members:**

Prof. Dr. Tülin Güray \_\_\_\_\_  
Biology Dept., METU

Prof. Dr. Ufuk Gündüz \_\_\_\_\_  
Biology Dept., METU

Assist. Prof. Dr. Bora Maviş \_\_\_\_\_  
Mechanical Engineering Dept., Hacettepe University

Assist. Prof. Dr. Dilek Keskin \_\_\_\_\_  
Engineering Sciences Dept., METU

Assist. Prof. Dr. Ayşen Tezcaner \_\_\_\_\_  
Engineering Sciences Dept., METU

**Date: 10.12.2009**

**I hereby declare that all information in this document has been obtained and presented in accordance with academic rules and ethical conduct. I also declare that, as required by these rules and conduct, I have fully cited and referenced all material and results that are not original to this work.**

Name, Last name: Gülseren Petek, Şen

Signature :

## ABSTRACT

### POLY (DL-LACTIC-CO-GLYCOLIC ACID) MICROPARTICLES AND SYNTHETIC PEPTIDE DRUG CONJUGATE FOR ANTI-CANCER DRUG DELIVERY

Şen, Gülseren Petek

M.S., Department of Biotechnology

Supervisor : Prof. Dr. Ufuk Gündüz

Co-Supervisor : Prof. Dr. Güngör Gündüz

December 2009, 98 pages

Cancer is a group of diseases in which normal cells are converted to cells capable of autonomous growth and invasion. In the chemotherapeutic control of cancer, drugs are usually given systemically so they reach toxic levels in healthy cells as well as cancer cells. This causes serious side effects. Another important problem with chemotherapy is resistance developed to cytotoxic drugs (multi drug resistance).

Doxorubicin (Dox) occupies a central position in the treatment of breast cancer. However doxorubicin induced cardiac toxicity is associated with a high incidence of morbidity and mortality. Resistance of malignant tumors to Dox is another important cause of treatment failure in patients with cancer.

One approach to overcome Dox-related toxicity is to use polymeric drug carriers, which direct the Dox away from heart tissue, and allow usage of lower dosages. In this present study two different anti-cancer drug delivery methods were evaluated. Dox was encapsulated in PLGA microparticles by single and double microemulsion solvent evaporation techniques. The highest entrapment of doxorubicin within PLGA microspheres obtained by optimization of process parameters. A sustained release of doxorubicin was obtained for 20 days.

Several protein transduction domains are known to have the ability to pass through biological membranes. One such peptide is HIV-1 TAT. In this study TAT was evaluated for its ability to carry Dox into Dox resistant MCF-7 tumor cells. Dox peptide conjugate was more potent than free drug. The concentration of drug in resistant cancer cells was increased indicating a partial reversal of drug resistance.

**Keywords:** PLGA, drug delivery, doxorubicin, protein transduction domain, multidrug resistance

## ÖZ

### ANTİ-KANSER İLAÇ TAŞINMASI İÇİN POLİ (LAKTİD-KO-GLİKOLİT) MİKROPARÇACIK VE SENTETİK PEPTİT-İLAC KONJUGASYONU

Şen, Gülseren Petek

Yüksek Lisans, Biyoteknoloji Bölümü

Tez Yöneticisi : Prof. Dr. Ufuk Gündüz

Ortak Tez Yöneticisi : Prof. Dr. Güngör Gündüz

Aralık 2009, 98 sayfa

Kanser hücrelerin kontrolsüz çoğalma ve yayılma özelliği kazandığı bir hastalıktır. Kanser kemoterapi ile tedavisinde ilaçlar genelde sistemik olarak verilir ve kan yolu ile vücuda dağılır. Ancak kanserli hücrelerin yanı sıra sağlıklı hücrelerde de ilaç seviyesi toksik düzeylere ulaştığında ciddi yan etkilere neden olmaktadır. Kemoterapi ile ilgili bir başka önemli problem de antikanser ilaçlara karşı gelişen dirençtir (çoklu ilaç direnci).

Doksorubisin (Dox) meme kanseri tedavisinde temel bir ilaç olmakla birlikte kalp hücrelerindeki toksik etkisi nedeniyle hastalık ve ölüm riskini arttırmaktadır. Tümörlerin Dox'a karşı direnç geliştirmeleri de kanserli hastalarda tedavinin başarısız olmasının önemli nedenlerinden biridir.

Dox'a baęlı toksisitenin önlenmesi için bir yöntem ilacın kalp kasını besleyen damarlara girmesini engelleyen ve düşük dozlar kullanılmasına imkan veren polimer ilaç taşıma sistemleri kullanılmasıdır. Bu çalışmada Dox, PLGA mikroparçacıklarına tekli mikroemülsiyon veya çiftli mikroemülsiyon çözücü buharlaştırma yöntemleri ile tutuklanmıştır. Farklı formülasyonlar oluşturularak en yüksek ilaç tutuklama miktarına sahip olan mikroküreler seçilmiştir. Yaklaşık 20 gün boyunca ilacı salma kapasitesi olan mikroküreler üretilmiştir.

Bazı virüslerin yüzeğinde bulunan proteinler hücre zarından geçebilme özelliğine sahip özel diziler içerirler. HIV virüsünün TAT peptidi böyle bir diziye sahiptir. TAT peptit kendisine tutturulmuş moleküllerin de hücre zarından geçebilme yeteneğini arttırmaktadır. Bu çalışmada TAT peptidinin Dox'u dirençli hücrelere etkili bir şekilde taşıdığı ve dirençli hücrelerde ilaç yoğunluğunu arttırarak ilaç dirençliliğinin kısmen önüne geçebildiği gösterilmiştir. Sitotoksikite çalışmaları Dox-TAT bileşiminin Dox dirençli MCF-7 tümör hücrelerinde serbest ilaçtan daha etkili olduğunu göstermiştir.

**Anahtar Kelimeler:** PLGA, ilaç taşıma sistemleri, doxorubisin, protein taşıma bölgeleri, çoklu ilaç dirençliliği

*To my family,*



## ACKNOWLEDGEMENT

I would like to thank all people who have helped and inspired me during my master study.

I especially want to thank my advisor, Prof. Dr. Ufuk Gündüz for adding me to her team, her friendship, advice, invaluable help, support and insight and my co-supervisor Prof. Dr. Güngör Gündüz for their guidance during my research.

I would like to thank Prof. Hidde Haisma for accepting me as a fellow researcher in his laboratory at University of Groningen. The associated experience broadened my perspective. Besides, he sets an example of a world-class researcher for his rigor and passion on research.

All my lab mates at METU made it a convivial place to work. I would like to thank Esra Kaplan, Zelha Nil for their friendship and help. Gülşah Pekköz, Gülistan Tansık, Tuğba Keskin and all the other folks had inspired me in research and life through our interactions during the long hours in the lab. It was fun to work with every undergraduate special student as well.

My deepest gratitude goes to my mother Sema, father Serdar and my sister Elif for their love and support throughout my life. I love you.

Last but not least, thanks to Hande Selamoğlu, İsmail Öğülür, Yaprak Dönmez, Derya Dilek, and Didem Coral for their great friendship and for all the fun we have had. Without them this thesis would not be possible.

## TABLE OF CONTENTS

ABSTRACT.....	iv
ÖZ .....	vi
DEDICATION .....	vi
ACKNOWLEDGEMENT .....	ix
TABLE OF CONTENTS.....	x
LIST OF FIGURES .....	xiii
LIST OF TABLES .....	xv
LIST OF ABBREVIATIONS .....	xvi
CHAPTERS	
1 INTRODUCTION .....	2
1.1 Cancer .....	2
1.1.1 Breast Cancer .....	3
1.1.2 Treatment Strategies for Breast Cancer .....	4
1.2 Doxorubicin .....	6
1.2.1 Mechanism of Action of Doxorubicin .....	8
1.3 Challenges in Chemotherapy Involving Anthracyclines .....	9
1.3.1 Anthracycline Induced Cardiac Toxicity .....	9
1.3.2 Multidrug Resistance .....	10
1.4 Controlled Drug Delivery Systems .....	11
1.4.1 Microparticle Based Polymeric Drug Delivery Systems .....	12
1.5 Protein Transduction Domains.....	15
1.5.1 TAT Protein Transduction Domain .....	15
1.6 Coupling Strategies to Link Cell Penetrating Peptides to Therapeutic Agents 18	
1.6.1 Restoring Free Sulfhydryl Groups for -SH Coupling .....	19
1.7 Protein Transduction Domains in Drug Delivery .....	21
1.8 Objective of the Study.....	22

<b>2</b>	<b>MATERIALS AND METHODS</b> .....	<b>23</b>
2.1	Materials.....	23
2.2	Cell Culture Propagation and Subculturing .....	24
2.3	Microparticle Preparation.....	25
2.3.1	Solvent Selection for Microparticles Preparation .....	25
2.3.2	Microparticle Preparation with W/O/W Double Emulsion Solvent Evaporation Method .....	26
2.3.3	Microparticle Preparation with O/W Single Emulsion Solvent Evaporation Method .....	28
2.4	Optimization of Encapsulation Process Parameters.....	28
2.5	Determination of Drug Encapsulation Efficiency.....	30
2.6	Drug Release .....	31
2.7	Drug Internalization Visualization.....	32
2.8	Dox-TAT Conjugation Reaction with SMCC.....	32
2.8.1	Quantification of Sulfhydryl Groups on TAT Peptide.....	33
2.8.2	Peptide Reduction .....	36
2.8.3	Activation of Doxorubicin .....	37
2.8.4	TAT Conjugation to Activated Doxorubicin .....	37
2.8.5	Following the Reaction with Thin Layer Chromatography .....	38
2.9	Purification of Dox-TAT Conjugate .....	39
2.10	Visualization of TAT Peptide on Tris Tricine SDS-PAGE .....	40
2.11	Cell Proliferation Assay .....	41
2.11.1	Cell Growth Inhibition of Microparticles .....	44
2.11.2	Cell Growth Inhibition of Empty Microparticles.....	44
2.11.3	Cell Growth Inhibition of Dox-Tat Conjugate.....	44
<b>3</b>	<b>RESULTS</b> .....	<b>45</b>
3.1	Microparticle Fabrication.....	45
3.2	Encapsulation Efficiency .....	45
3.3	Optimization of Encapsulation Parameters.....	46
3.3.1	Effect of PVA Concentration on EE .....	46

3.3.2	Effect of Volume Ratio of the Organic Phase to the Inner Water Phase on EE	47
3.3.3	Effect of Solvent Evaporation Time on EE.....	48
3.3.4	Effect of Emulsification Temperature on EE.....	49
3.3.5	Effect of First Emulsion Method on EE.....	49
3.3.6	Effect of Second Emulsion Time on EE .....	50
3.3.7	Effect of Theoretical Drug Loading on EE .....	51
3.3.8	Effect of Polymer Concentration on EE.....	52
3.3.9	Effect of Polymer Concentration on Size and Zeta Potential .....	54
3.4	Comparison of Microparticle Fabrication Methods.....	59
3.5	Morphology of Microparticles .....	59
3.6	Doxorubicin Release from Microparticles .....	61
3.7	Cell Proliferation Assay on PLGA Microparticles .....	66
3.8	Internalization of Doxorubicin Released from Microparticles .....	69
3.9	Dox-TAT Conjugation Reaction with SMCC.....	71
3.9.1	Activation of Doxorubicin .....	71
3.9.2	Quantification of Sulfhydryl Groups on TAT peptide.....	72
3.9.3	Reduction of Sulfhydryl Groups on TAT Peptide .....	73
3.9.4	TAT Conjugation to Activated Doxorubicin .....	75
3.10	Visualization of Dox-Tat Conjugate on Tris-Tricine SDS-PAGE.....	77
3.11	Purification of Dox-TAT Conjugate .....	78
3.12	Cell Growth Inhibition of Dox-TAT Conjugate .....	79
<b>4</b>	<b>CONCLUSION .....</b>	<b>81</b>
	<b>REFERENCES.....</b>	<b>82</b>
	<b>APPENDICES .....</b>	<b>94</b>
	<b>A. TRIS-TRICINE SDS-PAGE GEL BUFFERS.....</b>	<b>94</b>
	<b>B. SINGLE LETTER AMINO ACID CODES .....</b>	<b>96</b>
	<b>C. PROTOCOL FOR SILVER STAINING.....</b>	<b>97</b>

## LIST OF FIGURES

Figure 1 - Percent of all causes of death in Turkey (2004).....	3
Figure 2 - Chemical structure of doxorubicin .....	7
Figure 3 - Schematic presentations of W/O/W double emulsion droplets.....	13
Figure 4 - Chemical structure of polyvinyl alcohol (PVA) .....	14
Figure 5 - Domains of the HIV-1 TAT protein.....	17
Figure 6 - Structure of sodium borohydride.....	21
Figure 7 - Scheme for doxorubicin–TAT conjugate synthesis .....	33
Figure 8 - Reaction of Ellman's Reagent (DTNB) with sulfhydryls.....	34
Figure 9 - Thin layer chromatography schematic drawing .....	39
Figure 10 - 96-well plate cell seeding design for XTT assay .....	41
Figure 11 - 96-well plate drug application design for XTT.....	43
Figure 12 - Dox calibration curve in DMSO .....	46
Figure 13 - Effect of theoretical drug loading on EE.....	51
Figure 14 - Effect of PLGA concentration on EE.....	53
Figure 15 - DE microparticles' size distribution graphs .....	55
Figure 16 - Morphology of DE microparticles .....	60
Figure 17 - SEM images of doxorubicin loaded SE microparticles.....	60
Figure 18 - Calibration curve of doxorubicin in PBS .....	62
Figure 19 - Release profile of doxorubicin from microparticles.....	63
Figure 20 - MCF-7 cell proliferation profiles after incubation with SE particles.....	67
Figure 21 - MCF-7 cell proliferation profiles after incubation with DE particles.....	68
Figure 22 - Confocal microscopy analysis MCF -7 incubated with free doxorubicin	70
Figure 23 - Confocal microscopy analysis MCF -7 incubated with doxorubicin loaded SE microparticles.....	70
Figure 24 - Re-formation of sulfhydryl groups on TAT .....	74
Figure 25 - Thin layer chromatography of conjugation reaction products .....	75
Figure 26 - SDS-PAGE image of Dox and TAT .....	77

Figure 27 - Reaction Products on SDS-PAGE Gel.....	78
Figure 28 - Cell proliferation profiles of 600nm Dox resistant MCF-7 cell line after 72h incubation with Dox-TAT conjugate and free Dox .....	79

## LIST OF TABLES

Table 1 - Solubility of PLGA and Dox in several solvents.....	26
Table 2 - Effects of surfactant concentration EE .....	47
Table 3 - Effect of $V_o/V_{w1}$ on EE .....	47
Table 4 - Effect of solvent evaporation time on EE.....	48
Table 5 - Effect of emulsification temperature on EE .....	49
Table 6 - Effect of first emulsion method on EE .....	49
Table 7 - Effect of second emulsion time on EE .....	50
Table 8 - Effect of polymer concentration on zeta potential of DE microparticles ...	57
Table 9 - Effect of polymer concentration on mean size and zeta potential of SE microparticles.....	58
Table 10 - Tris-Tricine SDS-PAGE recipes.....	95

## LIST OF ABBREVIATIONS

DMSO	Dimethyl sulfoxide
dH <sub>2</sub> O	Distilled water
Dox	Doxorubicin
DDS	Drug delivery system
DLS	Dynamic light scattering
EE	Encapsulation efficiency
EDTA	Ethylenediaminetetraacetic acid
FBS	Fetal bovine serum
HLB	Hydrophile–lipophile balance
MPs	Microparticles
O/W	Oil in water
SE	Oil in water (O/W) single emulsion
PBS	Phosphate buffered saline
PLGA	Poly(dl-lactide-co-glycolide)
PVA	Polyvinyl alcohol
RT	Room temperature
SEM	Scanning electron microscopy
SMCC	Succinimidyl 4-[n-maleimidomethyl]cyclohexane-1-carboxylate
TL	Theoretical drug loading
TEA	Triethylamine
W/O/W	Water in oil in water
DE	Water in oil in water (W/O/W) double emulsion
XTT	Sodium(2,3-bis(2-methoxy-4-nitro-5-sulphophenyl)-2H-tetrazolium-5-carboxanilide proliferation assay



# 1 CHAPTER

## INTRODUCTION

### 1.1 Cancer

Cancer is the general name for a group of more than 100 diseases in which normal cells in a part of the body are converted to cells capable of autonomous growth and invasion. The adult human is composed of approximately  $10^{15}$  cells, many of which are required to divide and differentiate to repopulate organs and tissues which require cell turnover [1]. Variety of molecular mechanisms control cell multiplicity by balancing cell proliferation and apoptosis; cell death as the result of a programmed event. A whole series of genetic changes which may have taken many years to develop may alter this balance. This has the potential if not corrected to alter the total number of cells in a particular organ or tissue which normally never exceeds a fixed number. After many cell generations this increased cellular multiplicity would be clinically detectable as a tumor. Tumor cells differ from normal cells as they acquire some capabilities including, self-sufficiency in growth signals, insensitivity to antigrowth signals, resistance toward apoptosis, and limitless replicative potential [2]. Tumors can be either benign, arise in any tissue but do not travel to distance sites, or malignant (cancerous). Cancers are fully developed (malignant) tumors with a specific capacity to induce the formation of new blood vessels (angiogenesis), invade and destroy the underlying mesenchyme (local invasion) and then penetrate into lymphatic or blood vessels [3]. Most malignant cells eventually acquire the ability to metastasize. Metastasis is the spread of tumor cells and establishment of secondary areas of growth. Tumor cells can spread by three major routes. The first involves spread by direct extension of tumors in a body cavity, where as the second and third routes occur via the lymphatic and hematogenous compartments of the circulatory system [4].

Cancer is one of the leading causes of death worldwide. In Figure 1 the percent of all causes of death in 2004 in Turkey is given.

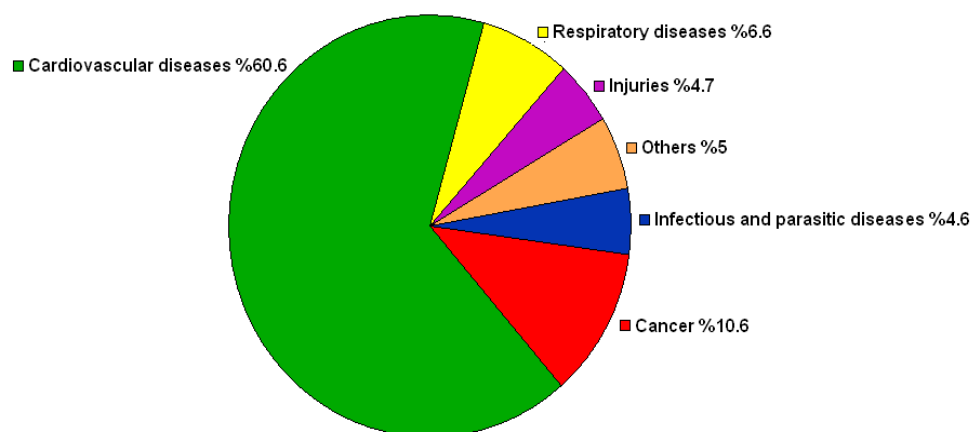


**Figure 1 - Percent of all causes of death in Turkey (2004)**

Data source: World Health Organization, Department of Measurement and Health Information, Mortality and Health Databases

There are many types of cancer. Bladder, breast, colon and rectal, endometrial, kidney, leukemia, lung, pancreatic, prostate, skin and thyroid are the most common ones. In 2008 breast cancer was the most leading site of new cancer cases among women [5,6]. Breast cancer alone is expected to account for 26% of all new cancer cases among women and continue to be the most common fatal cancer.

### 1.1.1 Breast Cancer

Breast cancer results from the malignant proliferation of epithelial cells lining the ducts or lobules of the breast. Breast cancer is a complex disease that is caused by both environmental and genetic risk factors. Although any women at any age can get breast cancer, it is primarily a disease of older age since over 90% of all diagnosed

cases are women older than 45 [7]. Macronutrient intakes, air and water pollutants, pesticides, radiation, alcohol, stress, oral contraceptives, hormonal therapies, obesity, abortions, age of first full time pregnancy are all thought to influence breast cancer risk [8]. Most breast cancers are sporadic (not inherited), but some are the result of inherited predisposition, principally due to mutations in the genes BRCA1 and BRCA2 [9, 10, 11]. BRCA1 and BRCA2 are caretaker genes that act as sensors of DNA damage and participate in DNA repair processes. The average cumulative risk of breast cancer at the age of 70 for BRCA1 and BRCA2 mutation carriers has been estimated to be up to 80% [12, 13]. Checkpoint kinase 2 (CHEK2) is an important signal transducer within the cellular network that responds to DNA damage and protects genomic integrity [14]. A specific variant of CHEK2 is identified to be conferring a moderate risk of breast cancer [15, 16]. Besides, the ataxia-telangiectasia (AT) gene, the TP53 gene, and the androgen receptor (AR) are now known to be responsible for inherited susceptibility to breast cancer [17]. The links in the causes are very complex. This makes the prevention very difficult and in most cases impossible. On the other hand, other big killers such as heart disease, HIV have clear paths to prevention.

Although treatment and early diagnosis has made a lot of progress in the past decades, breast cancer is still the most common form of cancer and cause of cancer related deaths among women. Therefore, much more research is needed to be done in breast cancer treatment.

### **1.1.2 Treatment Strategies for Breast Cancer**

There are three main treatments available; surgery, radiotherapy and chemotherapy. Surgery is successful for localized cancers and cancers at early stage. It involves the excision of the entire cancerous tissue together with adjacent tissues. For breast cancer, when the diagnosis is made, patients usually face the prospect of either breast conservation surgery (lumpectomy) or mastectomy. Mastectomy is the total removal

of a breast, where as lumpectomy is surgery in which only the tumor and some surrounding tissue are removed. Surgery is usually followed several weeks of chemotherapy and radiation therapy in order to remove any cancer cells left that may cause recurrence. Radiotherapy depends on the sensitivity of dividing cells to X-rays or gamma rays. However it has the risk of causing damage to the normal tissues in the irradiation field. While surgery is affective at early stages and limited to accessible tissues and radiotherapy is limited to sensitive cells, adjuvant therapy is used for treating metastatic diseases and preventing relapse. Adjuvant therapy is the use of systemic therapies (either chemotherapy or hormone therapy) in patients whose known disease has received local therapy but who are at risk of relapse. Several variables influence the response to systemic therapy. For example, the presence of estrogen and progesterone receptors is a strong indication for hormone therapy. On the other hand, patients with short disease-free intervals, rapidly progressive visceral disease, lymphangitic pulmonary disease, or intracranial disease are unlikely to respond to endocrine therapy [18].

Unlike many other epithelial malignancies, breast cancer responds to multiple chemotherapeutic agents. Chemotherapy is usually given systemically so the drugs are distributed to all over the body by the blood. Since the discovery of antiproliferative effect of mustard gas in 1945 [19] many drugs have been developed. Most of them are results of valuable discoveries by accident (i.e. mitoxantrone, originally intended as an ink) or by trial and error method as in the case of synthetic analogs of anthracycline antibiotic daunorubicin.

Anti-cancer drugs are divided into 6 classes according to their mode of action [20].

1. Alkylating agents whicc prevent cell replication by forming bonds with DNA, RNA, or certain proteins
2. Anthracycline antibiotics. Anthracycline intercalate between base pairs of DNA so disrupt cell replication and RNA transcription. The various

anthracycline analogues differ in their specificity for binding to DNA base sequences. These agents act specifically during the S phase of cell division. This group consists of the drugs; doxorubicin (adriamycin), daunorubicin, idarubicin, and epirubicin, and the synthetic mitoxantrone

3. Antimetabolites which are structural analogs of natural metabolites involved in DNA synthesis. Methotrexate, cytarabine, and 5-fluorouracil are antimetabolites.
4. Mitotic inhibitors with bind tubulin. Vincristine and vinblastine belong to this group.
5. Vinca alkaloids prevent tubulin polymerization and arrest cell division at metaphase.
6. Others, such as monoclonal antibodies and immunotoxins, and cancer-active hormones.

## **1.2 Doxorubicin**

Anthracycline is member of a family of chemotherapy drugs that are also antibiotics. Anthracyclines occupy a central position in the chemotherapeutic control of cancer. More than 90% of patients with locally advanced breast cancer show a better response to multidrug chemotherapy regimens that include an anthracycline.

The first anthracycline discovered was daunorubicin (daunomycin). Doxorubicin was developed shortly after [21]. Although there are marked differences in the clinical use of daunorubicin and doxorubicin, their chemical structures differ only by a single hydroxyl group on C14.

Doxorubicin is isolated from cultures of *Streptomyces peucetius var. caesius*. It has a broad spectrum of activity against neoplastic disease. It is an important drug in the treatment of hematologic malignancies, especially Hodgkin disease and the other

lymphomas [22]. The usual dose of doxorubicin when administered as a single agent by bolus intravenous injection is 60 to 75 mg/m<sup>2</sup> every 3 to 4 weeks.

Doxorubicin consists of daunosamine linked to a derivative of naphthacene (tetracene, an aromatic hydrocarbon consisting of 4 rings) through a glycosidic bond at ring atom 7. The structural formula is shown in Figure 2.

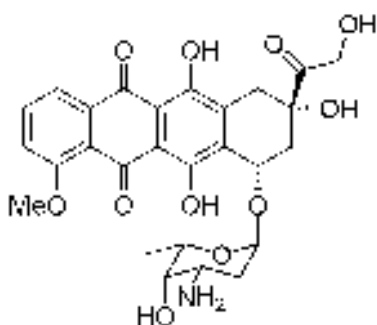


**Figure 2 - Chemical structure of doxorubicin**

The anthracycline ring is lipophilic, but the saturated end of the ring system contains abundant hydroxyl groups adjacent to the amino sugar, producing a hydrophilic center. The molecule is amphoteric, containing acidic functions in the ring phenolic groups and a basic function in the sugar amino group [23].

Doxorubicin is an essential component of treatment of breast cancer, childhood solid tumors, soft tissue sarcomas, bile ducts, endometrial tissue, the esophagus and liver, osteosarcomas, and aggressive lymphomas [24, 25]. While working with doxorubicin in the laboratory protective clothes and gloves should be used all the time. It is preferable to work in a designated area such as under a laminar flow system. The work space should be protected with disposable, absorbent paper. Spills can be cleaned with dilute (1%) HCl solution. All materials, including gloves must be placed in waste-disposal bin. Doxorubicin solution should not get into city sanitary

system. It should be put into toxic liquid waste bottle. In case of contact, skin should be thoroughly washed with soap and water or sodium bicarbonate solution. Brush should not be used. In cases of contact with eyes, the eye should be flushed with high amounts of water for at least 15 minutes while holding back the eye lids. Hands should be washed after removing the gloves.

### **1.2.1 Mechanism of Action of Doxorubicin**

Even though doxorubicin has been used over 30 years for the treatment of malignancies, its mechanism of action is uncertain. A number of different mechanisms have been proposed for the actions of anthracyclines. This includes;

1. Intercalation into DNA with consequent inhibition of macromolecular biosynthesis
2. Free radical induced DNA damage
3. Lipid peroxidation
4. DNA binding and alkylation
5. DNA cross-linking
6. Vinterference with DNA unwinding or DNA strand separation and helicase activity. By forming complex with topoisomerase II, they lead to double-stranded DNA strand breaks.
7. Alteration of membrane functions
8. Initiation of DNA damage via the inhibition of topoisomerase II [24, 25]

Doxorubicin binds to nucleic acids, presumably by specific intercalation of the planar anthracycline nucleus with the DNA double helix. However, there are contradictory findings regarding the involvement of DNA synthesis inhibition [26, 27, 28]. This effect maybe a transient component of drug action, while other effects such as the inhibition of topoisomerase II may be more closely associated with lethal

effects of the anthracyclines. These multiple mechanisms of action may be related to the utilization of different drug concentrations under varied experimental conditions.

### **1.3 Challenges in Chemotherapy Involving Anthracyclines**

#### **1.3.1 Anthracycline Induced Cardiac Toxicity**

Since their discovery at 1960s, anthracyclines remain some of the most effective anticancer drugs [21]. However anthracycline-induced cardiac toxicity is associated with a high reported incidence of morbidity and mortality. Especially doxorubicin induced cardio toxicity has dramatically hindered its usage [25, 30, 82].

The mechanism of the doxorubicin-induced cardio toxicity is not clear. Numerous mechanisms have been proposed. Major evidence suggests a correlation with the capacity to produce semiquinone free radicals and oxygen free radicals through an iron-dependent, enzyme-mediated reductive process [22, 31] which subsequently results in oxidative stress in cardiac tissue [33-36]. Other possible causes include; apoptosis, inhibited expression of cardiomyocyte-specific genes, and altered molecular signaling pathways [37].

Less doxorubicin induced cardiac toxicity may result from schedules that avoid high peak plasma concentrations, such as weekly doses (15–25 mg/m<sup>2</sup>) or continuous intravenous infusion over 48 to 96 hours [22]. Limiting the cumulative (lifetime) dose of to less than 450 mg/m<sup>2</sup> are shown to decrease cardio toxicity incidents. [38]. In order to minimize the total amount of Dox used, it is administered concurrently with other antitumor drugs such as vincristine, procarbazine, cisplatin and cyclophosphamide. Additional strategies that have been used in an attempt to prevent Dox-induced cardiomyopathy include the use of Dox analogues, alternative drug delivery systems, antioxidants, the iron chelator dexrazoxane, and combined



administration of the hematopoietic cytokines erythropoietin (EPO), granulocyte colony-stimulating factor (G-CSF), and thrombopoietin (TPO) [34].

Besides cardio toxicity, similar to other anticancer drugs targeting proliferating cell populations, doxorubicin causes significant gastrointestinal toxicity, with nausea, vomiting, diarrhea, and stomatitis that occurs within 7–10 days after administration. The typical acute dose-limiting toxicity for doxorubicin is that of a high incidence of myelosuppression, typically leukopenia and thrombocytopenia. In severe cases, this may lead to neutropenic fever and sepsis, requiring hospitalization [83].

### **1.3.2 Multidrug Resistance**

Clinical oncologists were the first to observe that cancers treated with multiple different anticancer drugs tended to develop cross-resistance to many other cytotoxic agents to which they had never been exposed, effectively eliminating the possibility of curing these tumors with chemotherapy. In many cases, cells grown in tissue culture from such multidrug-resistant tumors demonstrate patterns of resistance in vitro similar to those seen in situ. This observation suggests that multidrug resistance (MDR) is in many, but not all, cases the result of heritable changes in cancer cells causing altered levels of specific proteins, or mutant proteins, which allow cancer cells to survive in the presence of many different cytotoxic agents. These genetic alterations that confer resistance to cytotoxic drugs can affect cell cycle dynamics, susceptibility of cells to apoptosis, uptake and efflux of drugs, cellular drug metabolism, intracellular compartmentalization of drugs, or repair of drug-induced damage (usually to DNA). The best-studied mechanism of MDR is the over expression of an energy-dependent multidrug efflux pump, known as the multidrug transporter P-glycoprotein (P-gp) [32]. Doxorubicin is one of the most well know substrates of P-gp.

## 1.4 Controlled Drug Delivery Systems

For a drug to be effective it needs to reach to the site of action following administration (oral, intravenous, local, transdermal, etc.) at sufficient concentrations. The scientific field dealing with this issue is known as drug delivery and aims to deliver the drug at the site of action, at the right concentration for the right period of time. In case this is not accomplished by simply selecting an appropriate administration route, or if such administration causes patient discomfort, strategies based on delivering the drug with a carrier (a drug delivery system – DDS) are adopted. Novel DDSs present an opportunity to overcome the many challenges associated with drug therapy including poor solubility, tissue damage caused by drugs on extravasation, rapid breakdown and subsequent loss of action of the drugs in vivo. Poorly soluble hydrophobic drugs may precipitate in aqueous media and cause difficulties in achieving a convenient pharmaceutical format. DDS such as lipid micelles or liposomes provide both hydrophilic and hydrophobic environments, enhancing drug solubility. Neutral camptothecins [39], poorly water-soluble anti-inflammatory drug flurbiprofen [40], anti-cancer drug paclitaxel [41, 42] and docetaxel are among the drugs that are delivered by such carrier systems. Inadvertent extravasation of cytotoxic drugs leads to tissue damage as in the case of free doxorubicin [43].

Currently there are two liposomal doxorubicin formulations that are approved for clinical use: Doxil (Caelyx) and Myocet. The Doxil liposomal formulation is composed of hydrogenated soya phosphatidylcholine, cholesterol (Chol) and PEG-modified phosphatidylethanolamine. It is used primarily for the treatment of ovarian cancer. Myocet is composed of egg phosphatidylcholine (EPC) and Chol. It is used for metastatic breast cancer treatment. Myocet releases drug fairly rapidly and has a relatively short circulation lifetime. Doxil has a much longer circulation lifetime, which leads to large changes in biodistribution and particularly increased amounts of drug being delivered to the skin. This has advantages for the treatment of skin

localized cancers such as Kaposi's sarcoma but disadvantages in the observation of new dose-limiting toxicities such as the hand and foot syndrome [44].

#### **1.4.1 Microparticle Based Polymeric Drug Delivery Systems**

Micro emulsions are clear, stable, isotropic liquid mixtures of oil, water and surfactant. When these emulsions are hardened with solvent evaporation techniques they give rise to microparticles acting as reservoirs. They are potentially excellent carriers for bioactive molecules so thus a great interest for the pharmaceuticals research. Delivery of drugs using biocompatible systems are likely to provide protection from degradation, better absorption, by way of lower dose, reduced frequency of administration, and improved therapeutic index.

PLGA or poly(dl,lactic-co-glycolic acid) is a copolymer which is used in a host of Food and Drug Administration (FDA) approved therapeutic devices, owing to its biodegradability and biocompatibility. Depending on the ratio of lactide to glycolide used for the polymerization, different forms of PLGA can be obtained: these are usually identified in regard to the monomers' ratio used (e.g. PLGA 75:25 identifies a copolymer whose composition is 75% lactic acid and 25% glycolic acid. All PLGAs are amorphous rather than crystalline and show a glass transition temperature in the range of 40-60 °C. Unlike the homopolymers of lactic acid (polylactide) and glycolic acid (polyglycolide) which show poor solubility, PLGA can be dissolved by a wide range of common solvents, including chlorinated solvents, tetrahydrofuran, acetone or ethyl acetate.

##### **1.4.1.1 Single and Double Emulsions**

In double emulsions the droplets of one dispersed liquid are further dispersed in another liquid. The presence of a surfactant is often required to lower the interfacial

tension. There are two kinds of double emulsions;  $O_1/W/O_2$  (oil-in-water-in-oil) and  $W_1/O/W_2$  (water-in-oil-in-water).

The  $O_1/W/O_2$  double emulsion consists of small oil ( $O_1$ ) droplets dispersed in aqueous phase ( $W$ ) and this  $O_1/W$  emulsion itself is dispersed as large droplets in the continuous oil phase ( $O_2$ ).

The inner droplets ( $W_1/O$ ) and the droplets of the outer emulsion, also called as globules.  $O/W_2$  emulsion is stabilized by two separate layers of surfactants. Most double emulsions are prepared in two steps. At first, a high shear homogenization is applied on the system containing water, oil phase and hydrophobic emulsifiers. High shear and prolonged homogenization is needed in order to obtain small submicron water droplets and stable  $W_1/O$  emulsion. In the second step, the primary  $W_1/O$  emulsion is gently and slowly added to an aqueous phase containing the hydrophilic emulsifiers. Slow and stepwise addition under moderate stirring and without any high-shear homogenization should be applied [45].  $W/O/W$  double emulsions are very often used in the preparation of microspheres and other microencapsulated particles. Double emulsions will be referred as DE from now on. Figure 3 shows a schematic representation of  $W/O/W$  DE droplets.

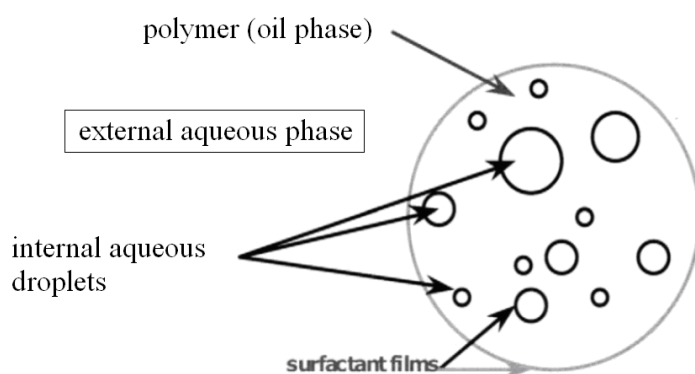


**Figure 3 - Schematic presentations of  $W/O/W$  double emulsion droplets**

In the case of the oil-in-water single emulsion (O/W emulsion), the oil is the inner phase, which is dispersed in the outer (water) phase. This is a one step process. Single emulsion will be referred as SE from now on.

Surfactants are classified as; anionic (negative charge), cationic (positive charge), zwitterionic or amphoteric (charge depends on pH) and non-ionic (no charge). All surfactants have both hydrophilic and lipophilic properties and are characterized by their hydrophile–lipophile balance (HLB) values. HLB system is the relationship (or balance) between the hydrophilic portions of the nonionic surfactant to the lipophilic portion. In general it applies to nonionic surfactants only. The HLB value is an indication of the solubility of the surfactant. The lower the HLB value the more lipophilic or oil soluble the surfactant is. And the higher the HLB value the more water soluble or hydrophilic the surfactant is. HLB values of the surfactants effect microparticles qualities. A high HLB surfactant can cause destabilization of the double structure while low HLB surfactant may lead to instabilities between globules. Surfactants with an HLB value >10 are predominantly hydrophilic and favor the formation of o/w emulsions, while surfactants with HLB values <10 are hydrophobic and form w/o emulsions [46]. HLB is an arbitrary parameter. Sometimes it is determined experimentally. For solubilizing oils (micro-emulsifying) into water, surfactant with HLB values of 13 to 18 are suitable. Polyvinyl alcohol (PVA) is a nonionic surfactant and has a HLB value of 18 [47]. In this study PVA is used as the surfactant. The hydrophilic group is polyhydric alcohol and the lipophilic group is fatty acid. It has an excellent emulsifying property. Figure 4 shows chemical structure of PVA.

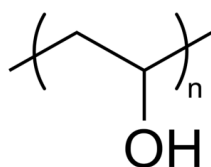


**Figure 4 - Chemical structure of polyvinyl alcohol (PVA)**

#### **1.4.1.2 Solvent Evaporation Technique**

Microparticles are prepared by the evaporation of the solvent within the microemulsion droplets. Enhancement in drug efficacy and lowering of drug toxicity could be achieved through encapsulation of the drug into these droplets.

### **1.5 Protein Transduction Domains**

Protein transduction domains (PTDs) have the ability to transduce or pass through biological membranes independent of classical receptor- or endocytosis-mediated pathways. One such peptide is TAT peptide human immunodeficiency virus type 1 (HIV-1).

#### **1.5.1 TAT Protein Transduction Domain**

One of the regulatory proteins encoded by HIV-1 is TAT which is a very powerful transactivator of HIV gene expression and essential for virus replication [61,62]. While the mechanism for transactivation is not known exactly, control of elongation by RNA polymerase II seems to be the main event [63]. Several earlier studies performed together and separately by Green, Loewenstein, Lillie et al., Pustai and Rawis at 1987 showed that only small regions of viral regulatory proteins are required for biochemical function. In one study performed by Green and Lowenstein (1988) boundaries of the functional domains of TAT peptide is defined by the analysis of C- and N- terminal deletion mutants. The study showed that the region from 37<sup>th</sup> amino acid to 57<sup>th</sup> is required and efficient for the transactivation by TAT peptides. Another important discovery of this group was demonstration of the full length 86 amino acid TAT protein is taken up by the cells when it is put directly into the medium. Transactivation effect proves that the TAT molecules are targeted to the nucleus after cytoplasmic delivery. This discovery raised the possibility of using TAT to deliver other macromolecules into cells. In 1988, Frankel independent from

Green also discovered that TAT protein was able to cross cell membranes. The first trials were done by conjugating B-galactosidase enzyme and horseradish peroxidase (HRP) to TAT (1-72) and TAT (37-72) [64]. They observed that cells treated with TAT conjugates revealed intense cellular staining, as an indication of cellular delivery and TAT (37-72) retains the cellular delivery function of TAT (1-72). In addition TAT (37-48) and TAT (47-58) were analyzed and found that they promote the uptake but showed cargo dependent variations in efficiency. A region of the TAT protein centered on a cluster of basic amino acids. All these peptides retain that basic domain (RKKRRQRRR) which is implicated in binding and uptake (see Appendix B for single letter amino acid codes). Figure 5 shows this basic domain. In 1997, Leblue et al. determined that the TAT (38-49) domain adopts an alpha helical structure with amphipathic characteristic, which is not required for cellular uptake, and reduce the efficiency of internalization induced by the basic domain. On the other hand, TAT (48-60) (GRKKRRQRRRPPQ) which contains the complete basic domain, fully retained cell internalization and nuclear accumulation, and showed no cytotoxic effects even at very high concentrations. This cluster of basic amino acids also thought to contain a nuclear localization signal (NLS) sequence. NLS causes the ever-open central channel of the pore (90 Å) to expand transiently up to 260 Å in diameter to allow nuclear protein entry (Powers et al., 1994). Although no definitive structure of regions important for nuclear localization for several viral proteins has been identified, a number of continuous positively charged residues are often present within the localization sequence [65, 66]. Therefore, the ability of cluster of basic amino acids of TAT to function as a nuclear localization or accumulation signal was investigated. GRKKR of TAT was observed predominantly in the nucleus. In contrast, the second stretch of positively charged amino acids including the sequence QRRP was for the most part localized in the cytoplasm [67, 69]. Therefore GRKKR sequence, or a part of basic domain, functions as a nuclear localization signal.

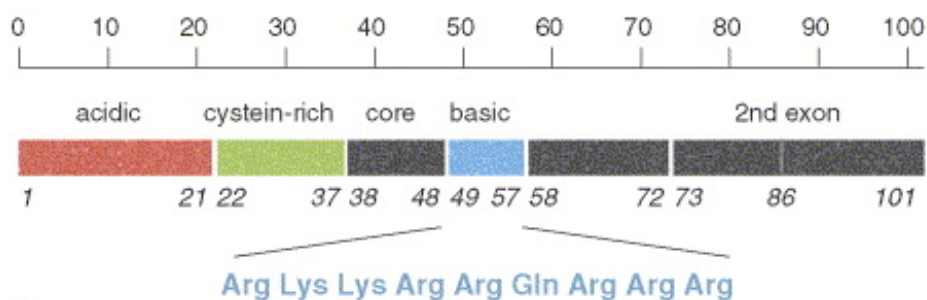


**Figure 5 - Domains of the HIV-1 TAT protein**

The mechanism of internalization of TAT protein is not clear. The observation that their internalization occurs at low temperature, in the absence of energy and only takes a few minutes led some authors to postulate that the mechanism of cell entry has to be receptor-independent and might imply the direct translocation of these molecules across the plasma membrane [70-72]. A hypothesis involves the tight ionic interactions between the basic groups of peptide side chains and the negative charges of the phospholipid heads could induce a local reorganization of the phospholipid bilayer. This would in turn lead to the formation of inverted micelles with the peptide enclosed in the hydrophilic cavity and finally the cytoplasmic release of the peptide. Then the nuclear localization signal causes TAT to be translocated into the nucleus and localize there [67]. According to this hypothesis since protein transduction is thought to target the lipid bilayer component of the cell membrane, so thus all mammalian cell types should be susceptible to import of proteins. It was also shown that TAT binds heparin through an interaction involving the basic domain of TAT. Heparin is a close structural homologue of the heparan sulfate (HS) glycosaminoglycan (GAG), a major constituent of cell surface and extracellular matrix proteoglycans, thus suggesting that membrane-bound HS proteoglycans (HSPG) might be involved in the TAT uptake and internalization process [69]. Several works on the other hand, showed that the internalization process occurs through caveolar endocytosis [73].



## **1.6 Coupling Strategies to Link Cell Penetrating Peptides to Therapeutic Agents**

Cell penetrating peptides can be biologically produced by using vectors expressing these peptides in cell culture. They can also be synthesized chemically. Solid phase peptide synthesis (SPPS) developed by R. B. Merrifield [48] was a major breakthrough in peptide chemistry. It allows the chemical synthesis of peptides and small proteins in the laboratory. The first stage of the technique consists of peptide chain assembly with protected amino acid derivatives on a polymeric support which is treated with functional units (linkers). The growing peptide in the solid-phase approach is linked to an insoluble support and therefore, after each reaction step, the byproducts are simply removed by filtration and washing. The second stage of the technique is the cleavage of the peptide from the resin support with the concurrent cleavage of all side chain protecting groups to give the crude free peptide [49, 50].

The TAT peptide used in this study was custom designed by a company.

Different strategies were developed to attach cell penetrating peptides to therapeutic agents such as drugs, drug loaded nanoparticles or liposomes. Terminal cysteine residues are added to the peptides during their synthesis. The sulfhydryl groups provided by cysteine residues can be coupled to another molecule in a specific orientation by using heterobifunctional crosslinkers [68]. This results in the formation of covalent thioether bonds (-S-C-) between two moieties and allows conjugation in a controllable fashion producing peptide molecules displaying the same basic confirmation. Since the cysteine residue is at the end, the majority of the peptide is free to interact with the cell membrane which is important for its internalization.

Heterobifunctional cross-linkers contain two different reactive groups that can couple two different functional targets. For example a cross-linker may contain a carbonyl-

reactive group on one end and a sulfhydryl-reactive group on the other end. Such a reagent might be used in conjugating carbohydrate-containing molecules with sulfhydryl-containing molecules. 4-(4-N-maleimido-phenyl) butyric acid hydrazide (MPBH) is such a cross-linker. Other types of cross-linkers can conjugate amine containing molecules to molecules with sulfhydryl groups. The amine reactive group is usually the active ester end having a group that can undergo nucleophilic substitution to form an amide bond with primary amines. The sulfhydryl reactive end is capable of creating either thioether or disulfide linkages. One such cross-linker is SMCC (Succinimidyl 4-[N-maleimidomethyl]cyclohexane-1-carboxylate). At least one reactive group of the cross-linker is more reactive and has greater stability in aqueous solutions. So reaction is usually performed in two steps.

Usually there is a spacer in between the two conjugated molecules. Conjugation reactions performed by using SMCC results in formation of an aliphatic cross-link containing a cyclohexane group. Conjugates may have different properties depending on the spacer. Some spacer may be immunogenic and cause specific antibody production [74].

SMCC is a widely used crosslinker for conjugation of biological moieties. It can be used to conjugate oligonucleotides to protein transduction domains (PTDs) to carry the DNA to the cell nucleus [75], for surface modification of liposomes [76,77] and reactive polymer films [78] and for direct covalent coupling of cytotoxic agents to peptides [79] and monoclonal antibodies [80] for naked antibody-targeted therapy.

### **1.6.1 Restoring Free Sulfhydryl Groups for -SH Coupling**

Chemically synthesized cysteine containing peptides are usually in their reduced form. However sulfhydryl groups are oxidized when the lyophilized peptides are reconstructed. Without reduction, dimers, trimers and tetramers may form. In addition, at higher concentrations peptides that have single or multiple free cysteines

will polymerize. If free sulfhydryl groups are not available, any chemical reaction involving free thiols will not be possible.

Trialkylphosphines are powerful and selective reductants for disulfides, but since they are not water soluble, they have not been commonly used in the life sciences. Dithiothreitol (DTT) and  $\beta$ -Mercaptoethanol (2-ME) are commonly employed to reduce disulfides [51, 52, and 53]. However these reagents contain thiols so they must be removed from the solution before the conjugation reaction. Usually gel filtration is performed, but TAT peptide used in this study has low molecular weight (1700Da). So gel filtration is not suitable. Alternatively TCEP•HCl, Tris (2-carboxyethyl) phosphine hydrochloride, rapidly and stoichiometrically reduces most peptide or other disulfides, even under acidic conditions [54]. Furthermore, aqueous solutions of TCEP are reasonably stable [55] and the functional concentration of TCEP is easily determined using DNTB. Even though TCEP does not contain any thiols, it reacts with electrophilic maleimides. Getz et al. found that TCEP inhibited the reaction of a peptide cysteine with a maleimide dye. So TCEP should also be removed after reduction. TCEP can be removed from solutions of cationic peptides by anionic ion exchange, with the peptide eluting in the flowthrough [56]. If excess TCEP remains, it is advantageous to couple at the highest acceptable pH to favor the reaction of the thiol over the TCEP [57]. Dialysis is another alternative to remove these reducing agents. However all of these methods require additional purification steps which are not possible sometimes (such as in the case of low molecular weight peptides) and these purification methods are often accompanied by air oxidation of the thiols back to the disulfides.

The most suitable method, for reducing the oxidized sulfhydryls for future use in cross-linking reactions involving small peptides, is using sodium borohydride ( $\text{NaBH}_4$ ) as the reducing agent [58, 59, 60]. Sodium borohydride is a milder reducing agent, can be used in aqueous solution. It acts specifically on disulfide bonds in peptides.

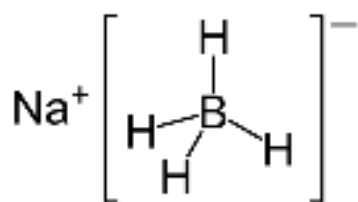


**Figure 6 - Structure of sodium borohydride**

### **1.7 Protein Transduction Domains in Drug Delivery**

PTDs also called cell penetrating peptides (CPPs) can facilitate the uptake of large, biologically active molecules into mammalian cells. Recent reports have suggested that PTDs may be able to mediate the delivery of cargo to tissues throughout a living organism. When these peptides are conjugated to drugs, as the cell culture and animal experiments have provided evidence, peptides can successfully transport drugs across the membranes of many different cell types. This may overcome bioavailability restriction imposed by the cell membrane. Furthermore cellular signals, such as nuclear localization signal, can be added to the peptide sequence so constructs can reach the interior of cells and interact with intracellular proteins. This is important for agents that are effective once they are inside the nucleus. PTDs are also used for the intracellular delivery of DNA. The use of PTDs for drug delivery represents a novel and promising approach [81].

## **1.8 Objective of the Study**

Objectives of the current study were to investigate PLGA microparticles for encapsulation and release of doxorubicin and study the effects of various formulation parameters on microparticles' characteristics and drug encapsulation.

Another aim was to synthesize doxorubicin–cell penetrating peptide conjugate with multidrug resistant tumor cell killing activity.

## 2 CHAPTER

### MATERIALS AND METHODS

#### 2.1 Materials

The biodegradable polymer poly (d,l-lactic-co-glycolic acid) (PLGA) used in encapsulation studies had a feed ratio of lactide to glycolide 75:25 with an average molecular weight (Mw) of 66,000-107,000, and purchased from Sigma (Germany). Polyvinyl alcohol (PVA) (MW: 30.000-70.000), Phosphate buffered saline (PBS) tablets were obtained from Sigma-Aldrich (Germany). Dialysis membranes (MwCo 1000, Diameter 26mm) were obtained from Serva (Germany).

The cross linker used in conjugation studies 4-(N-Maleimidomethyl) cyclohexanecarboxylic acid N-hydroxysuccinimide ester (SMCC) is purchased from AppliChem GmbH.

TAT Peptide, CYARAAARQARAG was custom synthesized by GenScript USA Inc, at a purity of >95%. See appendix B for single letter amino acid codes.

For cell culture, 0.25% Trypsin-EDTA solution, gentamycin sulphate, 0.5% trypan blue solution, XTT cell proliferation kit were purchased from Biological Industries, Kibbutz Beit Haemek (Israel). RPMI 1640 medium ((1x), 2.0g/l NaHCO<sub>3</sub> stable glutamine), fetal bovine serum (FBS) were obtained from Biochrom Ag. (Germany). Dimethylsulfoxide (cell culture grade), sodium dodecyl sulfate (molecular biology grade) were obtained from AppliChem (Germany). MCF-7 monolayer type human epithelial breast adenocarcinoma cell line was provided from Food and Mouth Diseases Institute (Şap) (Ankara). Doxorubicin.HCl (579.98g/mol) was kindly

donated by Prof. Dr. Fikret Apace and Prof. Dr. Ali Uğur Ural, Gülhane Military Medical School Hospital (Ankara).

## **2.2 Cell Culture Propagation and Subculturing**

MCF-7 cell cultures were propagated in RPMI 1640 medium. To make the complete growth medium, gentamycin to a final concentration of 1% and fetal bovine serum (FBS) to a final concentration of 10% were added to the base medium. The propagation atmosphere was %95 air and 5% carbon dioxide (CO<sub>2</sub>), and the temperature was 37.0°C.

Cells were cultured in T25 and T75 flasks. When the cells reached 70-80% confluence, they were passaged or subcultured. Both protocols involve; rinsing the cell layer twice with ½ diluted 0.25% (w/v) trypsin - 0.53 mM EDTA solution to remove all traces of serum which contains trypsin inhibitor. Then 0.25 and 0.5 ml of Trypsin-EDTA solution was added to T25 and T75 flasks respectively and placed at 37.0°C incubator until cell layer was dispersed. After complete dispersal, 4.0 and 8.0 ml of complete growth medium was added respectively to T25 and T75. Cells were resuspended by gently pipetting. Appropriate amounts of the cell suspension was left in the flask and remaining was discarded when a passage was desired or added to new culture vessels for subculturing. For MCF-7 cell line 1/3 passage ratio was found to be optimum. Higher ratios resulted in scattered cells while lower ratios lead to very densely populated flasks in a short time.

Cells, when not in use, were stored in freezing medium and kept at -80°C for short term storage and in the liquid phase of liquid nitrogen for long term storage. Cell freezing medium contains either 10 % DMSO in complete growth medium or FBS. For both of the freezing procedures first cells were trypsinized, and resuspended in freezing medium at 0°C. Since freezing medium contained DMSO it was harmful to cells above 0°C. Then cells were kept at -20°C for 1-2 hours before they were put

into -80°C. For long term storage cells were incubated at -80°C for overnight than placed in liquid nitrogen. For re-use, cells were thawed. 10 ml culture medium was put into a 15 ml centrifuge tube. Then the frozen cryotube vial was taken out of liquid nitrogen or -80°C and placed on the bench top to defrost. When almost liquid it was transferred to 15 ml tube and mixed carefully by flipping the tube. Cells were centrifuged at 500 rpm for 5 min then the supernatant was discarded and pellet was resuspended in fresh medium. Finally cells were transferred to cell culture flasks. For drug resistant MCF-7 cells, after thawing growth medium was enriched to have 20% FBS for the first days of culturing. Until the first passage doxorubicin is not added. Once resistant cells attach the surface of the flask and began to propagate then they were passaged in 1/2 ratio and doxorubicin was added afterwards.

## **2.3 Microparticle Preparation**

### **2.3.1 Solvent Selection for Microparticles Preparation**

According to US Patent 60/254,920 and 60/294,263 solvents with water solubility less than 5% are suitable for making microparticles (MPs) by solvent evaporation. The ability of these solvents to form a polymer membrane around the aqueous droplets depends on the surface tension. Solvents with high surface tension doesn't allow formation of stable polymer membrane, instead results in polymer precipitate. The table below shows the characteristics of some commonly used solvents.



**Table 1 - Solubility of PLGA and Dox in several solvents**

<b>Solvent</b>	<b>PLGA</b>	<b>Dox</b>	<b>Water solubility of Solvent (%)</b>
Water	I	S	N/A
Chloroform	S	P.I* S**	8
DCM	S	S	13
DMSO	S	S	100
Acetone	S	S	100
Ethanol	I	I	100

I: Insoluble, S: soluble

\*Doxorubicin in its protonated form \*\* Doxorubicin in its deprotonated form

For O/W SE method, a solvent which dissolves both PLGA and drug is required. DMF, DCM, DMSO, acetone and chloroform fits this criterion. However DMSO and acetone are highly soluble in water. Using these solvents would cause escape of doxorubicin to the outer aqueous phase. A solvent with lower water solubility is needed. In that case chloroform and DCM (methylene chloride) seems to be good options. Chloroform was used in this study due to its highly volatile nature. It added ease in solvent evaporation step.

For W/O/W DE method, doxorubicin was dissolved in water first then chloroform was used to dissolve PLGA.

### **2.3.2 Microparticle Preparation with W/O/W Double Emulsion Solvent Evaporation Method**

For the preparation of PLGA microparticles by W/O/W double emulsion method; Dox was dissolved in sterile dH<sub>2</sub>O. This makes the inner water phase. Erlenmeyer

flasks with magnet stirrers in them, tubes and every other material that can be autoclaved were autoclaved. PLGA was dissolved in chloroform to obtain the organic phase. Aqueous Dox solution was added into the organic phase and sonicated for 45 sec at 4 Amp on ice. This resulted in the first W/O emulsion phase. The polyvinyl alcohol as a solid was mixed in water to make a 2% surfactant solution. That is 4 grams of PVA per 196 grams (milliliters) of water. The best results were obtained by heating the water to about 80°C on a hot plate with magnetic stirrer. Temperatures above 80-90°C may result in decomposition of the PVA. The solution was cooled to RT and filtered through 20 µm filter by using a syringe. Surfactant solution was kept at 4°C and used within 2 days. Everything was pre-cooled at 4°C before encapsulation. In cold room (4°C), this primary emulsion was added drop wise by using a sterile syringe into the outer water phase containing 2% PVA under magnetic stirring at 1000 rpm. This emulsion is stirred for 10 minutes. Then the cap was opened and chloroform was evaporated completely. As the solvent evaporated, microparticles were hardened. Microparticles were obtained by centrifugation at 10000 rpm for 10 min at 4°C. Microparticles were washed with dH<sub>2</sub>O same amount as outer water phase (20 ml) to remove any residual-free drugs and -free surfactants. Washing step was repeated for three times. The PLGA microparticles were then lyophilized overnight, and kept in a sealed container at -80°C until use.

Unless otherwise mentioned, all the experiments were conducted by varying one of the parameters while keeping other processing parameters at a set of standard conditions: 20 ml 2% PVA solution the aqueous phase, 25 mg/ml PLGA in chloroform as the organic phase. Solvent volume was 1 ml (O). Doxorubicin was dissolved in sterile distilled water (W1) such that volume ratio of the organic phase( $V_o$ ) to water phase ( $V_{W1}$ ) was 20. Theoretical drug loading was 1%. Sonication of the first emulsion was done at 4 Amp for 45 seconds or until the solution becomes homogenous. Speed and duration of centrifuge for microparticle collection was 1000 rpm for 15 minutes.

### **2.3.3 Microparticle Preparation with O/W Single Emulsion Solvent Evaporation Method**

Dox was solubilized in chloroform ( $\text{CHCl}_3$ ) containing 5 M equivalent of TEA in respect to Dox at 1 mg/ml concentration. Solution was sonicated at 2 W for 5 min. The use of base (TEA) that deprotonates the Dox primary ammonium salt, induces the solubilization of Dox in  $\text{CHCl}_3$ . PLGA was dissolved in this solution to obtain the oil phase. This was added to the outer water phase as explained. All the other steps of microparticle preparation were same with double emulsion method.

Unless otherwise mentioned, all the experiments were conducted by varying one of the parameters while keeping other processing parameters at a set of standard conditions: 20 ml 2% PVA solution the aqueous phase, 8 mg/ml PLGA and 1 mg/ml doxorubicin were dissolved in chloroform as the organic phase. Solvent volume was 10 ml (O). Theoretical drug loading was 20%, sonication was done at 2 W for 5 minutes or until the solution becomes homogenous, speed and duration of centrifuge for microparticle collection was 1000 rpm for 15 minutes. Theoretical loading was 5% and emulsification steps were performed at room temperature (RT).

## **2.4 Optimization of Encapsulation Process Parameters**

One of the aims of this study was to evaluate the influences of concentration of the surfactant, amount of PLGA, ratio of volume of the organic phase to the volume of the inner water phase ( $V_o/V_{w1}$ ), solvent evaporation time, method of first emulsification (sonication vs. dispersion), emulsification time, rate of stirring during emulsification, temperature at which emulsification occurred, theoretical drug loading, on the microparticles' properties. The important properties of microparticles include; Dox entrapment efficiency (EE), particle size distribution, morphology, zeta potential, and drug release profiles. If we were to evaluate all of the possible process factors' effects on every single property then many experiments and analysis had to

be done. That would be very time consuming and expensive. So to begin with 6 factors; concentration of the surfactant, ratio of volume of the organic phase to the volume of the inner water phase ( $V_o/V_{w1}$ ), solvent evaporation time, method of first emulsification (sonication vs. dispersion), temperature at which first emulsification is done, second emulsification time, were chosen to be tested for their effect on EE. Size and surface properties are also important but they are somewhat more flexible and can be manipulated by changing several factors. However EE is one of the biggest limitations when water soluble drugs are tried to be encapsulated into micro carrier systems. So first these 6 factors were tried to be optimized in order to obtain the highest possible EE.

- To test the effect of concentration of the surfactant on EE, every experimental parameter except PVA concentration were kept constant. PVA concentration was changed from 1% to 2%.
- To test the effect of volume ratio of the organic phase to the inner water phase ( $V_o/V_{w1}$ ) on EE, instead of 500  $\mu$ l, same amount of drug was dissolved in 50  $\mu$ l. In the first case  $V_o/V_{w1}$  ratio was 5 (1000  $\mu$ l chloroform / 500  $\mu$ l water) and in the second case it was 20 (1000  $\mu$ l chloroform / 50  $\mu$ l water).
- To test the effect of solvent evaporation time on EE, instead of overnight solvent evaporation, solvent was only evaporated until no more phase difference was seen. That took almost 3 hours.
- To test the effect of emulsification temperature on EE, doxorubicin and PLGA solutions were mixed and allowed to be stirred under magnetic stirring for 5 hours at room temperature. Than during the preparation of another batch, these two steps were done at 4<sup>0</sup>C instead of RT.

- To test the effect of first emulsification method on EE, instead of dispersing the aqueous drug solution into PLGA solution the two phases were sonicated for 45 sec at 4 Amp on ice.

Second emulsification was done for 5 hours in the control group. To test the effect of time of second emulsification this was decreased to 10 minutes before the cap of the tube was opened and solvent was let to evaporate.

Then most appropriate formulations were selected for further evaluation to optimize other factors and obtain the best microparticle system in terms of particle size distribution, zeta potential and release properties.

## **2.5 Determination of Drug Encapsulation Efficiency**

The drug content in PLGA-MPs and the drug encapsulation efficiency (EE, %) were measured after extraction of drug from the microparticles. In order to extract Dox encapsulated in PLGA-MPs; Dox loaded and empty microparticles were weighted in triplicate (1 or 2 mg) and dissolved in 1 ml DMSO. Samples were vortexed and sonicated until the solution became clear. Each sample was divided into 200  $\mu$ l aliquots and put in each well of a 96 well plate. Absorption of the solution was measured in Elisa Plate Reader at 480 nm. Empty-MPs were used a blank. Standards were prepared from known concentrations of Dox in DMSO. Elisa plate was used to minimize the amount of MPs to be dissolved for EE experiment. It was also more accurate than measuring the doxorubicin absorbance by spectrophotometer because when Elisa was used it was possible to measure the absorbance of every sample at the same time under the same conditions. One the amount of drug was calculated equation 2.1 was used to EE and equation 2.2 was used to calculate the theoretical drug loading (TL, %).

$$EE \text{ (Encapsulation Efficiency, \%)} = \frac{\text{amount of drug inside MPs (mg)}}{\text{amount of drug initially used (mg)}} \times 100 \text{ (Eq. 2.1)}$$

$$TL \text{ (Theoretical Drug Loading, \%)} = \frac{\text{amount of drug (mg)}}{\text{amount of drug (mg) + amount of PLGA (mg)}} \times 100 \text{ (Eq. 2.2)}$$

## 2.6 Drug Release

Assessment of drug release from PLGA microspheres was done by sample and separate method, often referred to as the tube method. Doxorubicin loaded microspheres, 10 mg for each method in duplicates, were placed into 2 ml Eppendorf tubes containing 1 ml phosphate buffered saline (pH 7.4). Release was followed over a specified time. Samples were incubated in a horizontal shaker at 37°C, with continuous agitation at 200 rpm. Sampling was performed at predetermined intervals (1, 2, 3, 6, 7, 9, 10, 11, 14, 16, 17, 21, and 41 days) and isolation of the microspheres was achieved by centrifugation. The microsphere suspensions were centrifuged at 14000 rpm for 15 min. The clear supernatant (1 ml) was withdrawn and replaced with 1 ml fresh release medium. Upon centrifugation, settled microspheres were resuspended by vortexing. Supernatant was kept at -20°C until analyzing. The amount of doxorubicin released was determined by reading the absorbance of doxorubicin in Elisa Reader then calculating the concentration by using a standard curve of doxorubicin. Standard curve was prepared by dissolving known amounts of doxorubicin in PBS at pH 7.4 than reading the absorbance at 480nm. Microparticles were prepared for this experiment by using 8 mg/ml PLGA for SE and 80 mg/ml for DE method and the other experimental conditions were the same as given at section 2.3.2 and 2.3.3.

## **2.7 Drug Internalization Visualization**

In order to observe the drug internalization after being released from the SE microparticles confocal scanning electron microscopy analysis was performed. By using the emission wavelength of doxorubicin, the places of particles were detected easily without extra dyeing procedure. Cells were incubated on coverslips inside the wells of a six-well plate. First, coverslips were plated into wells and 3 ml of medium containing cells were poured onto wells (400.000 – 500.000 cells/well). Cells were waited to be attached onto coverslips in 24h. Necessary amounts of drugs were put in to the wells and waited for 1 hour, then washed three times with PBS and fixation was done with 70% ethanol for 10 minutes. Excess ethanol was removed by washing with PBS 3 times. Before removing the final PBS, coverslips were unattached from the bottom of the plates and put onto the slide upside down after pouring a drop of PBS on to slide. Slides were sealed by means of finger nail.

## **2.8 Dox-TAT Conjugation Reaction with SMCC**

SMCC was used to conjugate amine containing doxorubicin molecules to TAT peptides with C-terminal cysteine residues. The reaction was performed in several steps. Reaction scheme is shown below in Figure 7.

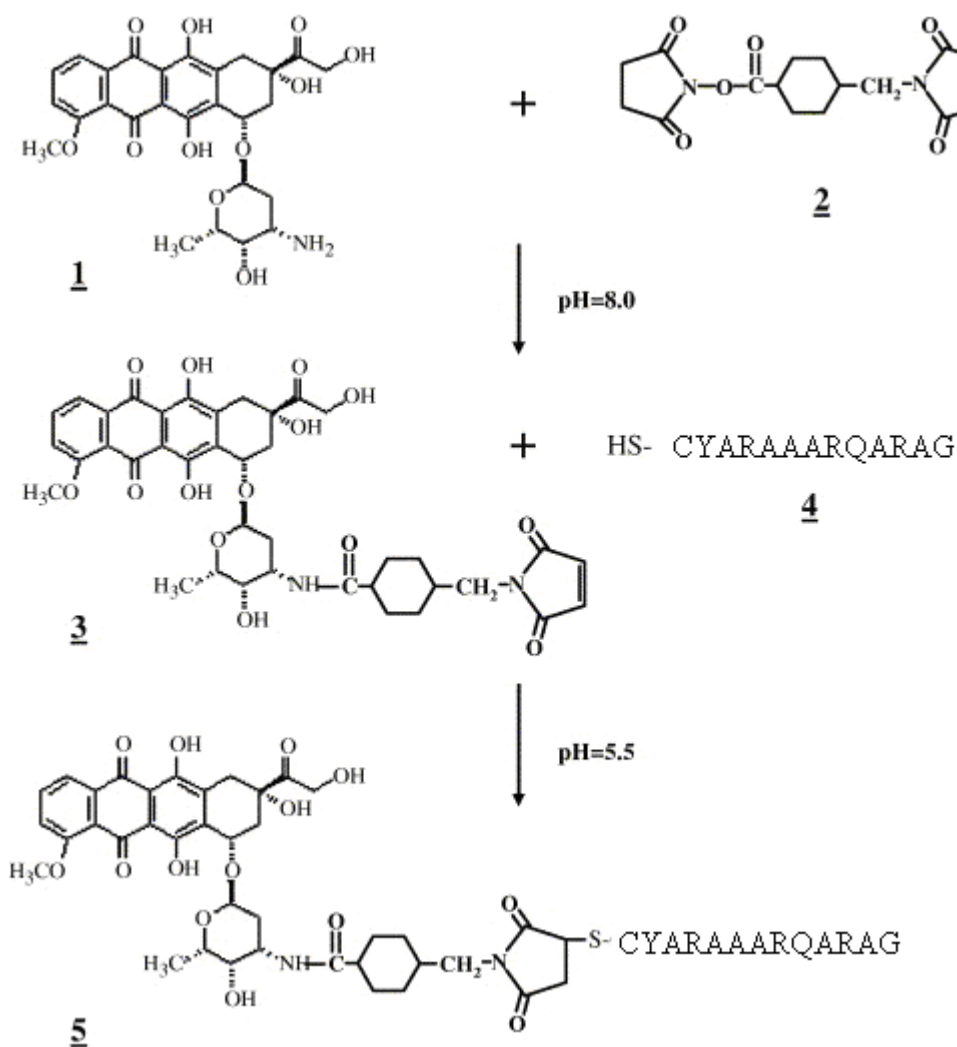


**Figure 7 - Scheme for doxorubicin-TAT conjugate synthesis**

1, doxorubicin; 2, SMCC; 3, doxorubicin-SMCC; 4, TAT peptide; 5, doxorubicin-TAT conjugate

### 2.8.1 Quantification of Sulphydryl Groups on TAT Peptide

It is important to know the concentration of free sulphydryl groups before starting to the reaction. Free -SH groups were quantified by the DTNB method (Ellman 1959).



A solution of DTNB (5, 5'-dithio-bis-(2-nitrobenzoic acid)), also called Ellman's Reagent, produces a mixed disulfide and 2-nitro-5-thiobenzoic acid (TNB) when it reacts with free sulfhydryls [85]. The Figure 8 shows the reaction of DTNB with a -SH. While DTNB has little, if any absorbance, TNB is a yellow colored product and has a high molar extinction coefficient in the visible range. This reaction is rapid and stoichiometric, with the addition of one mole of thiol releasing one mole of TNB. Consequently, Ellman's Reagent is very useful as a sulfhydryl assay reagent because of its specificity for -SH groups at neutral pH, high molar extinction coefficient and short reaction time.

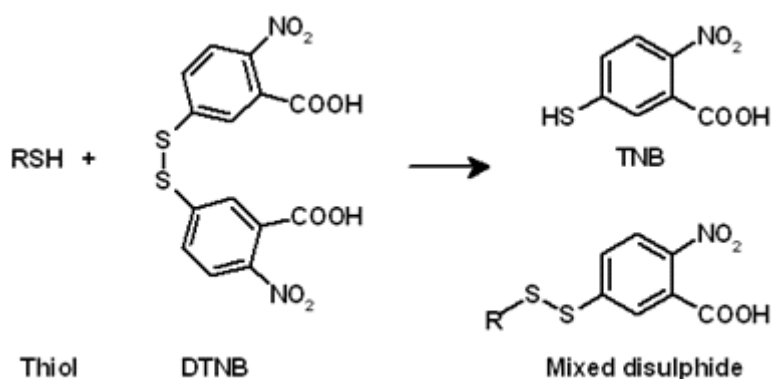


**Figure 8 - Reaction of Ellman's Reagent (DTNB) with sulfhydryls**

The molar extinction coefficient of TNB is reported to be  $14,150 \text{ M}^{-1}\text{cm}^{-1}$  at 412 nm [86, 87] in 0.1 M phosphate buffer containing 1 mM EDTA at pH 8.0. The extinction coefficient was used to calculate the number of sulfhydryl groups must be matched to the reaction conditions.

There are two methods of quantitating sulfhydryl groups. One is by comparison to a standard curve composed of known concentrations of a sulfhydryl-containing

compound such as cysteine, and the other is by taking the extinction coefficient of TNB as a reference. Second approach was adopted in this study.

Procedure for quantitating sulfhydryl groups based on molar absorptivity was performed according to Pierce instructions. Solutions below were prepared and used;

- Reaction buffer: 0.1 M sodium phosphate, 1 mM EDTA at pH 8.0
- Ellman's Reagent Working Solution: 4 mg Ellman's Reagent dissolved in 1 ml of reaction buffer. The unused portion was stored at 4°C for a maximum of two weeks for future use.
- Peptide sample 2: 2 µl TAT stock solution (19 mg/ml) was added to 2.748 ml reaction buffer + 50 µl Ellman's Reagent solution
- Blank: 2.750 ml Reaction buffer + 50 µl Ellman's Reagent solution

The above solutions were prepared. Ellman's Reagent was added last. Solutions were incubated at RT for 15 minutes. At the end of the incubation spectrophotometer was set to 412 nm and zero on the blank. The absorbance of the peptide sample was measured. The amount and concentration of sulfhydryls in the samples were calculated from the molar extinction coefficient of TNB ( $14,150 \text{ M}^{-1}\text{cm}^{-1}$ ).

Molar absorptivity,  $E$ , is defined as follows:

$$E = A / (bc)$$

where  $A$  = absorbance,  $b$  = path length in centimeters,  $c$  = concentration in moles/liter (=M)

The concentration in the spectrophotometric cuvette was calculated from the formula:

$$c = A / (bE)$$

The concentration of the assay solution (2.8 ml) was calculated by multiplying with the dilution factor. From the molarity values, moles of sulfhydryl in the assay solution were calculated. These moles of sulfhydryl in the assay solution were contributed by the original 2  $\mu$ l sample. Therefore, the concentration of free sulfhydryl in the original unknown sample was calculated with linear proportion.

### **2.8.2 Peptide Reduction**

Cysteine residues on TAT peptide will invariably polymerize upon reconstitution from their lyophilized form. A detailed protocol on reduction with sodium borohydride is given by James Gailit (1993) in his paper about restoring free sulfhydryl groups in synthetic peptides. A modified form of that procedure was followed in this study.

Reaction buffer for DTNB assay was adjusted to pH 9.8 with NaOH. Peptides were dissolved in this solution to the final concentration 1 mg/ml. At this time point an aliquot was taken and analyzed with Ellman's Reagent as described above. Dry NaBH<sub>4</sub> was added to final concentration of 0.1M NaBH<sub>4</sub> and solution was mixed slowly to avoid foaming. Cap was left loose. A stream of argon gas was passed over the reaction vessel slowly and constantly. At t=15, 30, 60, 90, 120 minutes aliquots were taken. Borohydride will reduce DTNB so every sample that contains NaBH<sub>4</sub> was acidified with 0.5 M HCl for 10 min before analysis. Since DTNB color should be developed in a mild alkaline environment, the pH of the reaction mixture was brought back to pH 8.0.

Aliquots were analyzed by DTNB method. When absorbance stopped to increase the solution was acidified back to pH 4.0 using dilute HCl and incubated at RT for 10 min to stop the reaction. Quantization of sulfhydryl groups in the final mixture was calculated as described in the section 2.8.1 “Quantification of Sulfhydryl Groups on TAT Peptide”.

### **2.8.3 Activation of Doxorubicin**

The amine reactive N-hydroxysuccinimide (NSH-ester) undergoes a nucleophilic substitution to form an amide bond with the primary amines of doxorubicin molecules. In the first step 0,9 mg doxorubicin was dissolved in 500  $\mu$ L DMSO and dispersed in 2 ml conjugation buffer (0.1 M sodium phosphate, 0.150 M sodium chloride, pH 7.2)

20  $\mu$ L TEA was added and pH was adjusted back to 8.0. Then 0.5 mg SMCC was added to the solution. Final volume was filled up to 3 ml with conjugation buffer. Reaction proceeded for 2 hours at gentle mixing (200 rpm) at RT, under argon atmosphere and protected from light.

### **2.8.4 TAT Conjugation to Activated Doxorubicin**

225  $\mu$ l sulfhydryl- (cysteine residue) containing TAT (19 mg/ml) was added to the reaction mixture. The addition of thiols to maleimides occurs via a Michael addition and is usually performed at a low pH due to the base-catalyzed ring opening of the maleimide [88]. Sulfhydryl containing peptide can be added in excess to the amount of maleimide activity present on the drug. 1.5 fold molar excess was used. This second step of the reaction must be performed below pH 7.5 to prevent hydrolyzation of the maleimide end. Reaction was carried under argon atmosphere and protected from light.

### 2.8.5 Following the Reaction with Thin Layer Chromatography

To analyze maleimide activation of doxorubicin after the first reaction and TAT conjugation to the activated doxorubicin after the second reaction very small samples of reaction mixtures were taken with a capillary before beginning to the reaction and after each reaction. Solvent systems 1:1 ethanol: chloroform was found to be appropriate from thin layer chromatography (TLC). As stationary phase, a silica coated metal film as a thin layer (~0.25 mm) was used. A start line 1 cm from the bottom of the plate and a stop line 1 cm below the top of the plate were drawn with a pencil. Free doxorubicin, doxorubicin activation reaction mixture and TAT conjugation reaction mixture were spotted at three far apart dots on the start line. A small amount of 1:1 ethanol: chloroform solvent mixture (mobile phase) was placed in a closed container as it was below the start line. A filter paper was placed inside the container to have a concentrated solvent mixture. The lower edge of the plate was then dipped in the solvent. Solvent travels up the matrix by capillarity, moving the components of the samples at various rates because of their different degrees of interaction with the stationary phase and solubility in the developing solvent. When solvent reached the stop line, plate was removed and air dried. Since doxorubicin is a colored substance no other visualization technique was required. Doxorubicin and the reaction products were seen as red spots on the TLC plate. The spots were circled to have a permanent record how far the compound travelled on the plate. The products from two subsequent reactions which were visible as separated spots were identified by comparing the distances they have travelled with those of doxorubicin. The distance of the start line to the solvent front (stop line) was measured (b) and divided by the distance of centre of the spot to the start line (a). The resulting ratio is called retardation factor ( $R_f$ -value).

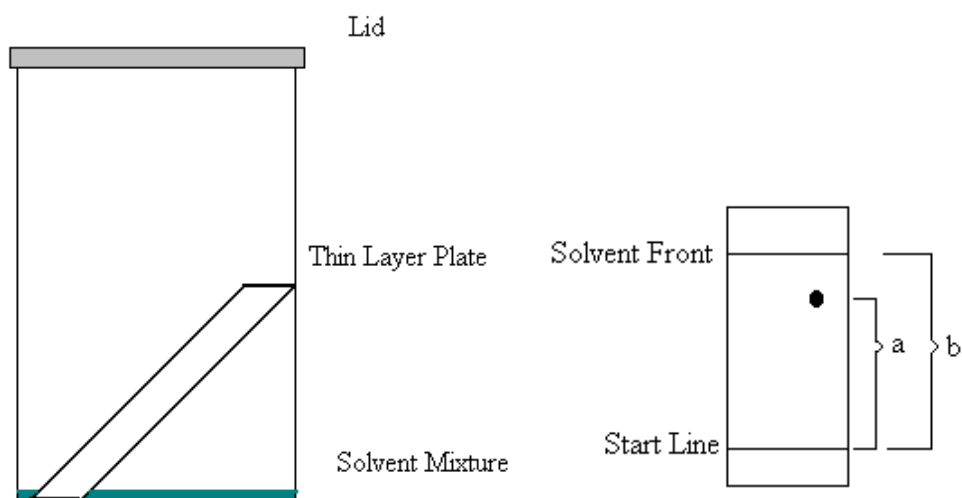


**Figure 9 - Thin layer chromatography schematic drawing**

$R_f$  value is ratio of the distance the solvent travels to the distance compound travels  
 $(R_f = a/b)$

## 2.9 Purification of Dox-TAT Conjugate

To remove small molecules; unreacted Dox, SMCC and TEA from Dox-TAT conjugate reaction mixture was dialyzed by using a tubing with molecular cut of 1000. To prepare the dialysis tubing 0.9306 gram of EDTA was dissolved in 250 ml water (10 mM) at pH 5.5. Then pH was adjusted back to 7.5 with NaOH. Tubing was boiled in this solution for 30 minutes. Then 10 mM EDTA solution was diluted to 1 mM to have the storage solution. Dox-TAT reaction mixture (3ml) was put into tubing and both ends were sealed. Dialysis was done against 100 ml PBS over night at 4°C, making three buffer changes.

## **2.10 Visualization of TAT Peptide on Tris Tricine SDS-PAGE**

Tris-SDS-PAGE is commonly preferred to separate proteins and peptides in the mass range 1-15 kDa. The recipes for gel buffers, cathode and anode buffers are given in Appendix A.

To prepare sample buffer; 0,3634 g Tris (121,14 g/mol) was dissolved in 9 ml dH<sub>2</sub>O (pH ~10). Then 10 M HCl was added until pH was 7.0 (~500 µl). Volume was filled up to 10 ml. 0.6 g SDS was dissolved in this solution. 6 ml glycerol was mixed while preventing formation of bubbles. Eventually 10 mg Coomassie Brilliant Blue was added and solution was divided into two (8 ml each). For reducing sample buffer 600 µl mercaptoethanol and 1400 ml dH<sub>2</sub>O, for non-reducing 2 ml dH<sub>2</sub>O was added.

5 µl sample buffer was added to 15 µl peptide sample. Samples were incubated at 37<sup>0</sup>C for 15 min. Gels were mounted and anode (red) buffer was added as the lower electrode buffer and cathode (black) buffer was used as the upper electrode buffer. Samples were loaded under the cathode buffer. Maximum 10 µL of samples were loaded.

Protein bands containing a minimum of 0.2 µg of protein are suitable for Coomassie Staining. In that case using a protocol that contains no methanol is preferred. Hundred fold smaller proteins can be visualized by silver staining. Both methods were tried to visualize TAT peptides. Silver staining was found to give the best result. First gels were treated with fixing solution to fix the proteins to the gel matrix and avoid protein diffusion. Then gels were washed to remove acetic acid coming from the fixer solution. Then gels were washed in pre-treatment solution which contains sodium thiosulfate. After washing with silver nitrate solution protein bond silver ions were reduced by developing solution. By this method even slightest peptide on the gel could be visualized. Detailed silver staining protocol is given in Appendix C.

## 2.11 Cell Proliferation Assay

XTT, 2, 3-bis (2-methoxy-4-nitro-5-sulfohenyl)-2H-tetrazolium-5-carboxanilide, is a tetrazolium derivative. XTT is reduced by of mitochondria enzymes in live cells. XTT is readily reduced to a highly water-soluble orange colored product. The amount of water-soluble product generated from XTT is proportional to the number of living cells in the sample and it is quantified by measuring absorbance at wavelength of 500 nm.

These mitochondria enzymes were inactivated shortly after cell death. So XTT Cell Viability Assay determined live cell number based on the activity of mitochondria enzymes in live cells. Determination of live cell number was used to assess rate of cell proliferation and to screen cytotoxic effect of doxorubicin and its TAT conjugate.

For the assay 96 well plates were used. On day 1, 5000 cell/well were seeded to the wells marked below. The other wells were left empty.

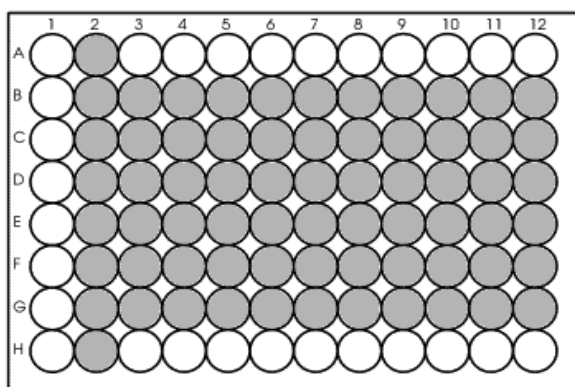


**Figure 10 - 96-well plate cell seeding design for XTT assay**



For counting, cells were trypsinized and homogenized as it is done in subculturing. Appropriate amount of cell suspension containing 10% Tryphan blue solution was prepared.

Cells were counted using hemocytometer (HHH, Germany) under light microscope. The smallest center square on hemacytometer has  $0.00025 \text{ mm}^3$  volume. To calculate the number of cells in  $1 \text{ cm}^3$ ,  $4 \times 10^6$  coefficient number was used in calculation. The number of the cell/ml was calculated by the formula given below:

Cell number/ml= average count per square x dilution factor x  $4.10^6$  (Eq. 2.3)

After 24 hours cells were attached to the surface of the well and recovered from the possible negative effects of trypsinization. At day 2, medium was removed by flipping the plate upside down. 150  $\mu\text{l}$  fresh medium was added to all of the wells except the wells of the 3<sup>rd</sup> column.

Then, highest dose of drug, drug-conjugate, drug containing and empty MPs were added to the 3<sup>rd</sup> column in 300  $\mu\text{l}$ . 1/2 serial dilutions were applied horizontally. The Figure 11 shows the final organization.

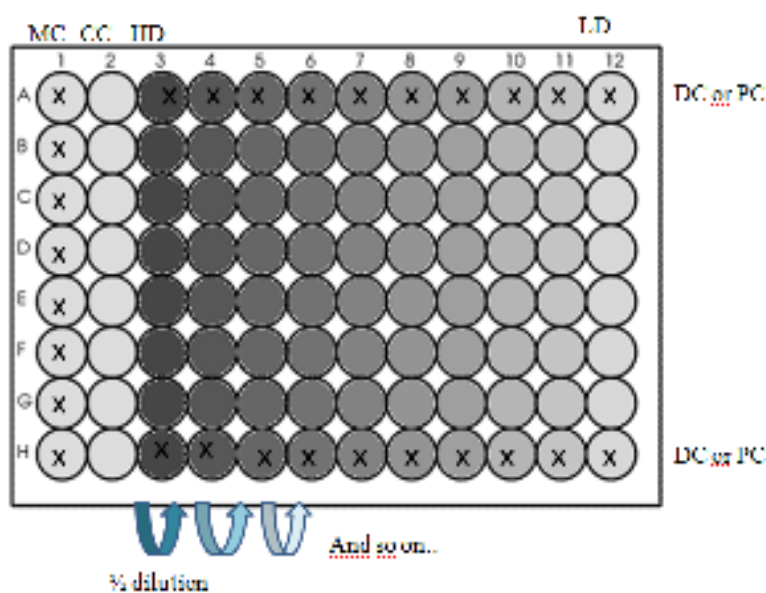


**Figure 11 - 96-well plate drug application design for XTT**

Cross (x) marks indicate the wells that lack cells. MC: medium control; nothing but complete growth medium, CC: cell control; No cytotoxic reagent, only 5000cells/well, HD: highest dose, LD: lowest dose, DC: drug control, PC: empty MP control

Plates were incubated in humidified CO<sub>2</sub> incubator at 37°C for 72h. By the end of the incubation, XTT and activator reagents were applied to each plate and plates were incubated in dark for 4-5 h. The intensity of the color change was measured by using ELISA reader (SPECTRAmax 340PC) at 500 nm.

Viability curves of cells in each plate were determined by considering the intensities of each well subtracting from the intensity of control groups (medium control, cell control and empty microparticle control). From the proliferation curves the half maximal inhibitory concentration (IC<sub>50</sub>) was determined. It is a measure of the effectiveness of a compound in inhibiting biological or biochemical function. It indicates how much of a particular compound was needed to inhibit a given biological process (or component of a process) by half. IC<sub>50</sub> value of the samples was

calculated by using the logarithmic equation of the viability curves. All the experiments were done in triplicates.

### **2.11.1 Cell Growth Inhibition of Microparticles**

According to the protocol at section 2.11 MCF-7 cells were incubated for 72h in  $\frac{1}{2}$  serial dilutions of doxorubicin loaded microparticles prepared by both SE and DE methods. Encapsulation process conditions were same as the standard conditions except the polymer concentration in the organic phase. In SE particles 8 mg/ml PLGA was used and in DE particle 40 mg/ml PLGA was used. 150  $\mu$ M doxorubicin containing microparticles were dispersed in cell culture medium and used as the highest dose for each of the methods.

### **2.11.2 Cell Growth Inhibition of Empty Microparticles**

According to the protocol at section 2.11 MCF-7 cells were incubated for 72 h in  $\frac{1}{2}$  serial dilutions of empty microparticles having the highest dose of 1.66 mg/ml and lowest dose of 0.003 mg/ml. Following the incubation, XTT assay was performed. Empty MPs used in cytotoxicity assay experiments were produced under same conditions with the ones containing drug. Conditions are explained in previous section. Empty particles had same volume of solvent without drug.

### **2.11.3 Cell Growth Inhibition of Dox-Tat Conjugate**

Both sensitive and resistant MCF-7 cells were seeded in 96 well plates. 5  $\mu$ M free and TAT conjugated doxorubicin was used as the highest dose.  $\frac{1}{2}$  serial dilutions were performed in each column and XTT assay was done according to the protocol at section 2.11.

## **3 CHAPTER**

### **RESULTS**

#### **3.1 Microparticle Fabrication**

Doxorubicin was encapsulated in PLGA micro particles by single (O/W) and double (W/O/W) micro-emulsion techniques. Several process factors were optimized to achieve maximum entrapment efficiency. The best formulations with the highest drug encapsulation efficiencies were further investigated for their size distribution, zeta potential, and drug release profiles.

#### **3.2 Encapsulation Efficiency**

Drug encapsulation efficiency is the ratio of the amount of drug loaded to microparticles to that of the amount of the drug initially used. The encapsulation efficiencies of microparticles were calculated by using Equation 2.1. In order to determine the doxorubicin concentration, a calibration curve of standard doxorubicin solution in DMSO was prepared first. Calibration curve was linear over studied range with a correlation coefficient of  $R^2 = 0.9993$ .

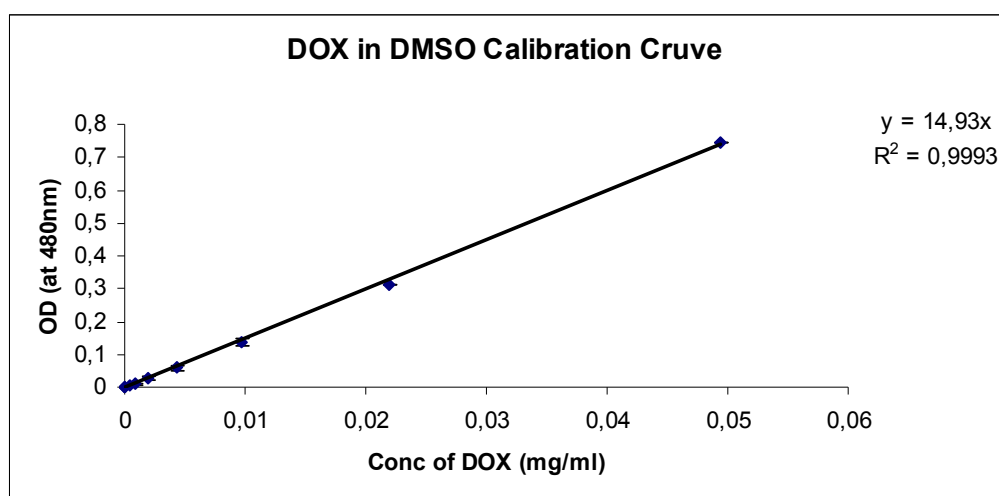


**Figure 12 - Dox calibration curve in DMSO**

For all of the different batches of microparticles encapsulation efficiencies were calculated by extracting the drug inside the microparticles then measuring its absorbance at 480 nm then calculating the corresponding concentration from the calibration curve at Figure 12.

### 3.3 Optimization of Encapsulation Parameters

#### 3.3.1 Effect of PVA Concentration on EE

Two different PVA concentrations in the outer water phase were evaluated in terms of their effect on encapsulation efficiency. Every other process parameters were kept constant. 1% PVA concentration resulted in low entrapment efficiency (10.2%). When PVA concentration was doubled to 2% entrapment efficiency increased two folds as well (21.02%). Results are shown in Table 2.

**Table 2 - Effects of surfactant concentration EE**

<b>PVA (%)</b>	<b>EE (%)</b>
1	10.2
2	21.02

PVA was needed as a stabilizer to prevent coalescence of the emulsified droplets. It decreases the surface tension between the organic and aqueous phase during microparticle preparation. Increase in PVA concentration also increases viscosity of external water phase. This in turn would increase the diffusional resistance to drug molecules so prevent drug losses to the external aqueous phase. Drug losses occurring during emulsification process is the main cause of low encapsulation efficiencies. Increasing the PVA concentration decreased the drug loss so increased encapsulation efficiency. This effect has also been observed by other authors [94].

### **3.3.2 Effect of Volume Ratio of the Organic Phase to the Inner Water Phase on EE**

$V_o/V_{w1}$  is the ratio of volume of the organic phase to the volume of the inner water phase.  $V_o/V_{w1}$  ratio of 20 vs. 5 were compared for their effect on EE.

**Table 3 - Effect of  $V_o/V_{w1}$  on EE**

<b><math>V_o/V_{w1}</math></b>	<b>EE (%)</b>
5	13.32
20	16.41

Higher  $V_o$  to  $V_{w1}$  ratios mean that less water was used to dissolve the drug. This is in agreement with the results reported previously (Kissel et al., 2007). Increase in EE might have resulted from less aqueous drug solution got in contact with outer water phase so less drug molecules escaped to the aqueous phase. Studies of Chaderi et al., and Schlicher et al. at 1997 on PLGA microparticles-FITC dextran system revealed that low volumes of  $W_1$  phase resulted in a minimal microporosity of the polymer matrix, whereas high  $W_1$  volumes caused an increasing number of micropores and channels thereby facilitating the rapid initial diffusion of encapsulated drugs. In conclusion higher  $V_o/V_{w1}$  resulted in higher EE.

### 3.3.3 Effect of Solvent Evaporation Time on EE

Solvent was evaporated until no more phase difference was visible. That took almost 3 hours when 1 ml of solvent was used.

**Table 4 - Effect of solvent evaporation time on EE**

<b>Solvent Evaporation Time</b>	<b>EE (%)</b>
Over night	13.32
3 hours	28.2

The effect of decreasing solvent evaporation time on the EE was expected because the less the particles stayed in aqueous solutions the less they loose their encapsulated water loving drug. The solvent was removed by evaporation at room temperature. Evaporation could have done under vacuum to shorten the process. That might cause less drug leakage to the outside PVA solution.

### 3.3.4 Effect of Emulsification Temperature on EE

Doxorubicin and PLGA solutions were mixed and allowed to be stirred under magnetic stirring for 5 hours at room temperature. To test the effect of temperature every other parameter kept constant only these two steps were done at 4°C instead of RT. Table 5 shows the effect of decreasing temperature on EE.

**Table 5 - Effect of emulsification temperature on EE**

<b>Solvent Evaporation Temperature</b>	<b>EE (%)</b>
Room Temperature	13.32
4°C	22.3

As it is known that a high loading of a hydrophilic drug can only be expected from a stable emulsion [95]. At approximately 4°C, water reaches its maximum density. At 4°C more stable emulsion must have been produced which in turn aided encapsulation of drug.

### 3.3.5 Effect of First Emulsion Method on EE

Instead of dispersing the aqueous drug solution into PLGA solution the two phases were sonicated for 45 sec at 4 Amp on ice.

**Table 6 - Effect of first emulsion method on EE**

<b>1<sup>st</sup> Emulsion Method</b>	<b>EE (%)</b>
Dispersion	13.32
Sonication	26.8



High shear and prolonged homogenization is needed in order to obtain small submicron water droplets and stable W<sub>1</sub>/O emulsion [84]. When drug solution was dispersed in organic phase by vortex the formed emulsion was not stable and two phases were separated after some time. The shear stress produced by vortex might not be enough to produce a stable emulsion. However when they were sonicated a homogeneous mixture was formed which remained stable until the second emulsification step. That might be the reason of high encapsulation efficiencies of microparticles prepared by performing sonication in the first emulsification (W<sub>1</sub>/O) step.

### 3.3.6 Effect of Second Emulsion Time on EE

Time of second emulsification is the time passes from the injection of polymer phase into 2% PVA phase until the time when the cap of the tube was opened and solvent was let to evaporate.

**Table 7 - Effect of second emulsion time on EE**

<b>2<sup>nd</sup> Emulsion Time</b>	<b>EE (%)</b>
5 hour	13.32
10 min	37.07

The reduction in encapsulation efficiency with prolonged stirring times have been previously observed [96].The less the microparticles stay in aqueous phase in which drug has much greater solubility, the higher the encapsulation efficiencies. Anything that decreases the contact time of particles with water minimizes drug diffusion to the outer phase so increase encapsulation efficiency.

### 3.3.7 Effect of Theoretical Drug Loading on EE

Figure 13 shows the effect of theoretical drug loading (%) on encapsulation efficiency for microparticles produced by double and single emulsion methods.

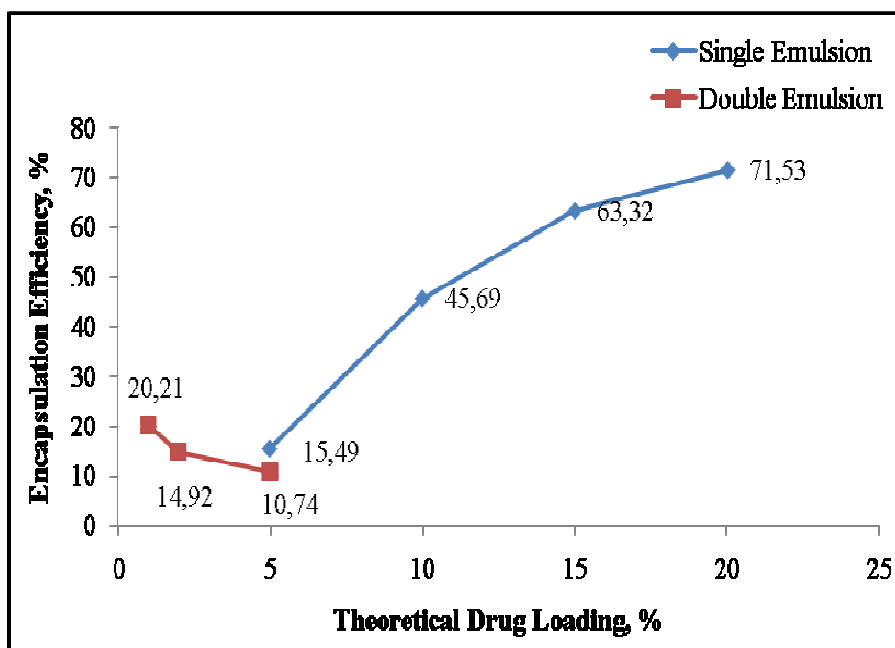


Figure 13 - Effect of theoretical drug loading on EE

Theoretical drug loading (TL) was increased while keeping the other parameters constant. In SE particles EE increased at higher TL values. Changing TL from 5% to 20% increased EE from 15.49% to 71.53%. This shows that as more drug was added it's incorporated into the particles. On the other hand, changing TL resulted in an opposite effect in microparticles produced by DE method. The increase in TL from 1% to 5% resulted in a decrease of EE from 20.21% to 10.74%. To understand whether drug incorporation decreases we need to know the drug content. The decrease in EE might have resulted from the saturation of the polymer with drug.

Drug content would stay the same while EE decreases when a fixed amount of drug is going into the particles in spite of increasing drug input.

It is also possible that increasing TL would increase drug loss during microencapsulation process. Increasing drug loading resulted in decreased encapsulation efficiencies in DE method. This is observed by other authors as well in PLGA nanoparticle systems encapsulating hydrophilic drugs [97-99]. In DE method drug and polymer were in water and chloroform respectively. These are immiscible with each other. The increased amount of Dox in water would increase the concentration gradient between two phases. Drug molecules within the polymer matrix are attracted towards the doxorubicin molecules in the aqueous phase and migrate to the aqueous phase.

In SE particles on the other hand, it is obvious that saturation of the polymer was not achieved at low theoretical drug loading values so drug content kept increasing as more drug was added. In SE method, drug and polymer were dissolved in the same solvent and almost a homogenous solution was formed. Encapsulation of drug depends on its interaction with the polymer. There are limited numbers of functional groups on PLGA that can interact with doxorubicin molecules. As more drug molecules were added more interactions must had been formed, so encapsulation was increased. After some time that increase would stop as well when all the available functional groups were occupied.

### **3.3.8 Effect of Polymer Concentration on EE**

Figure 14 shows the effect of PLGA change in the organic phase on EE of microparticles prepared with single emulsion and double emulsion solvent evaporation methods.

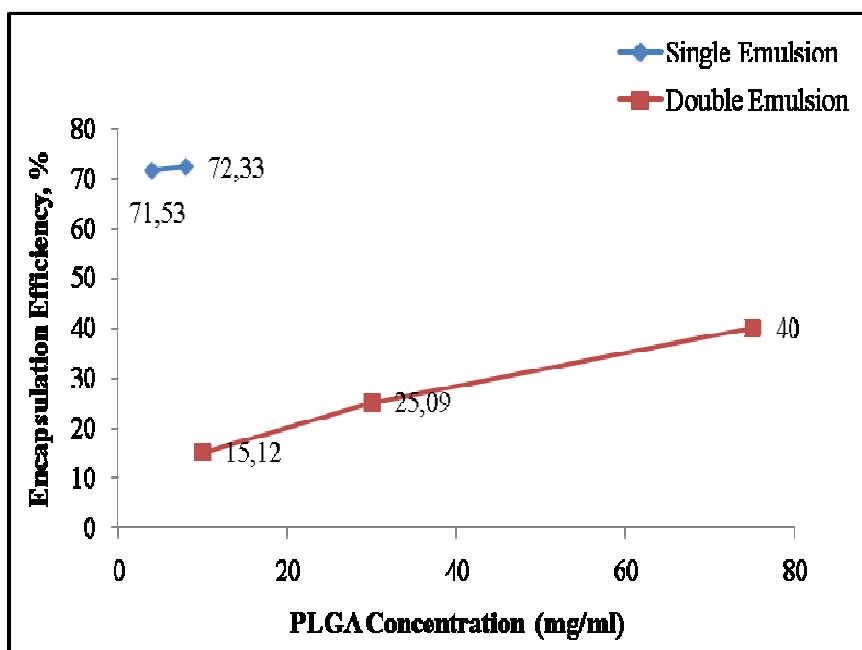


**Figure 14 - Effect of PLGA concentration on EE**

During fabrication of SE microparticles, PLGA concentration was increased from 4 mg/ml to 8 mg/ml. PLGA concentration could not be increased further while keeping TL high because solubility of doxorubicin in chloroform is very low when compared to its solubility in water. Increasing the PLGA amount would lead to decreased TL values because drug can not be added to the same extent. PLGA concentration increase resulted in a minor increase in EE. This might indicate that SE microparticles were saturated for drug. In contrast, change in polymer concentration on three batches of DE microparticles lead to increased EE values. 10 mg/ml, 30 mg/ml and 75 mg/ml PLGA was used. This behavior was also observed by other authors [100]. When polymer concentration was increased further (100 mg/ml) organic phase became too viscous and prevented microparticle formation (results not shown).

The increase in the concentration of the polymer would result in a corresponding increase in viscosity that directly influences the stability of the emulsion and therefore the encapsulation of the hydrophilic Dox molecules increased. The increased organic phase viscosity, increases diffusional resistance to drug molecules from organic phase to the aqueous phase, thereby entrapping more drug in the polymer microparticles. Also the time required for polymer precipitation decreases at higher polymer concentrations, so there is less time for drug molecules to diffuse out of microparticles, which increases the drug content. These results were also observed by other authors [101, 102].

### 3.3.9 Effect of Polymer Concentration on Size and Zeta Potential

The size distribution of MPs was analyzed by DLS. Size distribution obtained as a plot of the relative intensity of light scattered by particles in various size classes and is therefore known as an intensity size distribution. Software uses Mie theory for conversion of the intensity distribution into volume and number [103]. The graphs in Figure 15 show the effect of polymer concentration in the organic phase on the size distribution of particles.

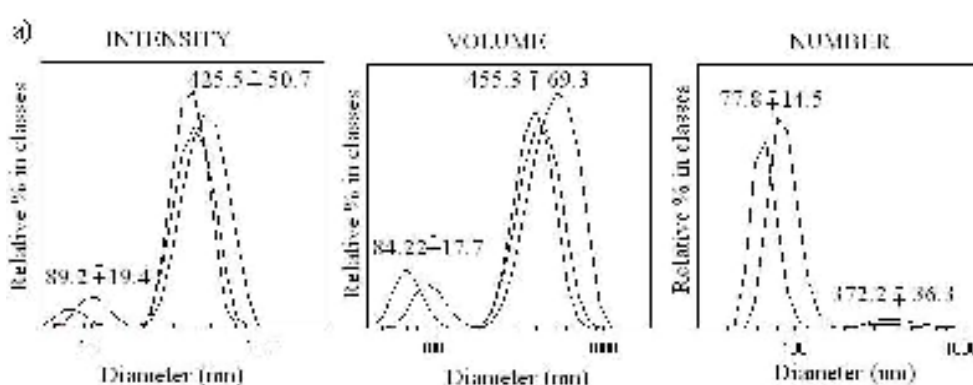


**Figure 15 - DE microparticles' size distribution graphs**

a) DE-4 (10 mg/ml PLGA)

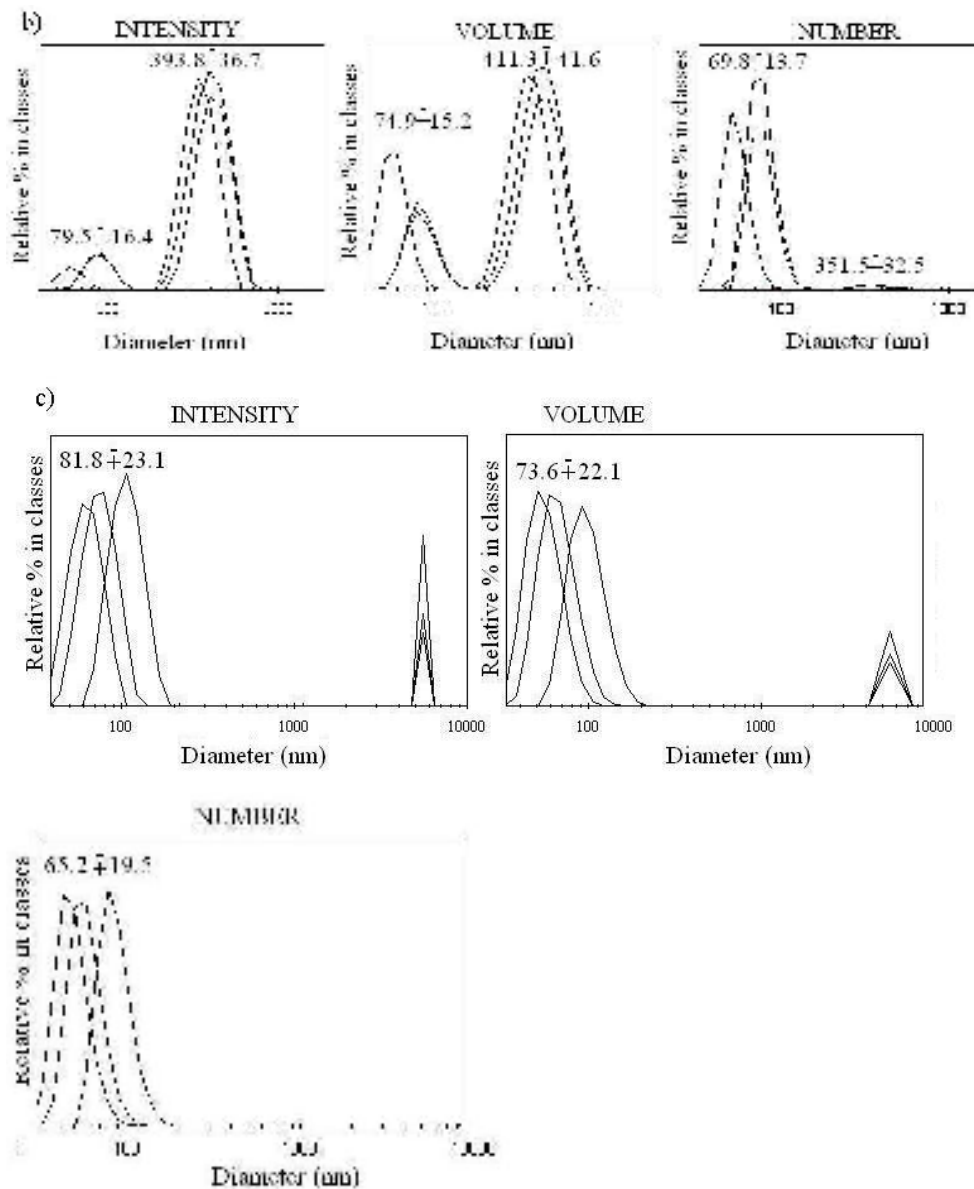


**Figure 16 - DE microparticles' size distribution graphs (continued)**

b) DE-5 particles (30 mg/ml PLGA) c) DE-6 (75 mg/ml PLGA) size distribution by intensity, volume and number

Figure 15 shows size distribution graphs obtained by three measurements. Mean diameters and standard deviations are given on the graphs. Results show that the

increase in polymer concentration from 10 mg/ml to 30 mg/ml and 75 mg/ml was resulted in limited change on the particle size. At 75 mg/ml PLGA concentration one of the two subgroups had very large particles ( $>5\mu\text{M}$ ). But these were in minority. Bimodal population might have resulted from using less PVA than required. PVA might not be enough to prevent coalescence of formed particles. Large particles might have resulted from poor polymer dispersion into water due to high viscosity of the organic phase. The increase in the particle size with increasing drug polymer concentrations has been observed by other authors for PLGA polymers [104, 105]. This was probably caused by the increasing viscosity of the dispersed phase (polymer solution), resulting in poor dispersibility of the PLGA solution into the aqueous phase. There is likely to be higher viscous resistance against the shear forces during the emulsification [106].

For each of size distributions (by intensity, volume and number) there was a different mean value. That is because intensity distribution of bimodal or broad monomodal dispersions is greatly affected by the scattering angle so that a different mean diameter is mostly obtained by volume and number.

Only for perfectly monodisperse samples will the number, volume and intensity weighted average particle size can be similar. As the polydispersity of the population increases, the averages become more distinct from each other. Thus the number average decreases whereas the intensity average increases on increasing peak broadening [107]. Prepared microparticles had high polydispersity index values.

The mean size of particles is an important property. Nanoparticles are mainly used for their cellular targeting ability following systemic administration, while microparticles have been used for many years as controlled release delivery systems for drugs and therapeutic proteins. However going from micro to nano may bring some problems along. Intravenously administered nanoparticles generally become associated with organs of the reticuloendothelial system (RES), mainly the liver and

spleen [89,90]. This tendency restricts the ability of nanoparticles to be directed to specific target tissues. Microparticles have longer circulation times, and hence greater ability to target to the site of interest. Moreover microparticles offer the advantage of a higher payload especially for hydrophilic drugs in particles, and a better ability to provide a controlled release. [91]. Majority of the particles prepared in this study was smaller than 500 nm. Interestingly SEM images show much larger particles. The diameter that is measured in DLS is a value that refers to how a particle diffuses within a fluid so it is referred as a hydrodynamic diameter. Ionic strength of the medium, surface structure, density will produce different mean sizes and size distributions. Even the size in a microscope image will depend on parameters set such as edge contrast. It is important to understand that none of these results are inherently "correct". SEM shows diameter of dry particles.

Besides size, PLGA concentration change might have an effect on zeta potential as well. In Table 8 microparticles prepared by double emulsion solvent evaporation method are given in terms of changing PLGA concentrations and corresponding zeta potentials.

**Table 8 - Effect of polymer concentration on zeta potential of DE microparticles**

<b>PLGA concentration (mg/ml)</b>	<b>Zeta (mV)</b>
10	-31 ±0.98
30	-28.8 ±3.0
75	-32.5 ±2.54

Results indicate that polymer concentration did not effect zeta values significantly in microparticles prepared by DE method. Results are average of three successive readings.



Table 9 shows the effect of PLGA change on mean size and zeta potential of nanoparticles prepared by single emulsion solvent evaporation method.

**Table 9 - Effect of polymer concentration on mean size and zeta potential of SE microparticles**

<b>PLGA concentration (mg/ml)</b>	<b>Mean Size (nm)</b>	<b>Zeta (mV)</b>
4	474.7±18.0	-1.6 ±1.5
8	395.7±92.2	-10.46 ±0.28

Again change in PLGA concentration did not results in a significant change in particle size but it increased zeta potential. Zeta potentials give information about the stability of suspension. High values indicated that there would be high repellent forces between particles and this would prevent aggregation. The magnitude of the zeta potential, which determines the charge at the boundary of the diffuse region situated around the Stern layer (one of two electrically charged layers of electrolyte ions, the layer of ions immediately adjacent), gives an indication on the stability of a colloidal system. SE method produced particles with lower zeta values. SE microparticles' zeta potential values were between 10 and -10 mV which leads to the conclusion that microparticle suspensions would not be very stable over time. For this reason, particles were stored as a lyophilized powder and resuspended upon need. In addition to stability, the surface charge of the particles might be an important factor in predicting the in vivo degree of interaction with the cell surface and thus the degree of microparticle uptake by the cells.

### **3.4 Comparison of Microparticle Fabrication Methods**

The maximum entrapment efficiencies accomplished were 40.0 % and 72.3 % for DE and SE methods respectively. Highest encapsulation efficiencies were accomplished by SE method. The low entrapment of Dox in DE method could be explained by preferential localization of drug at the outer aqueous phase rather than inside the nanoparticle core, which was less hydrophilic. In DE method drug and polymer were in different solvents that are immiscible with each other. Some drug partitioned into the aqueous medium during the emulsification and the evaporation of the organic solvent steps. In addition, some drug was lost in the repeated washings of the microspheres with water during the harvesting and extraction process. On the other hand in SE method, Dox was solubilized in chloroform which is immiscible with water, so its escape to the outer phase was minimized. In SE method, drug and polymer were dissolved in the same solvent and almost a homogenous solution is formed. Panyam (2004) and Budhian (2005) reported that higher drug polymer miscibility leads to higher drug incorporation. This might be the reason of higher drug contents achieved by SE method.

SE solvent evaporation method is a one step process so it is easier and takes less time.

### **3.5 Morphology of Microparticles**

The shapes of microparticles prepared by SE and DE methods were studied under light microscope and scanning electron microscope (SEM). Both of the imaging techniques revealed considerable differences in the shapes and surface characteristics of microparticles. Figure 16 and 17 show the light microscope and SEM images of MPs.

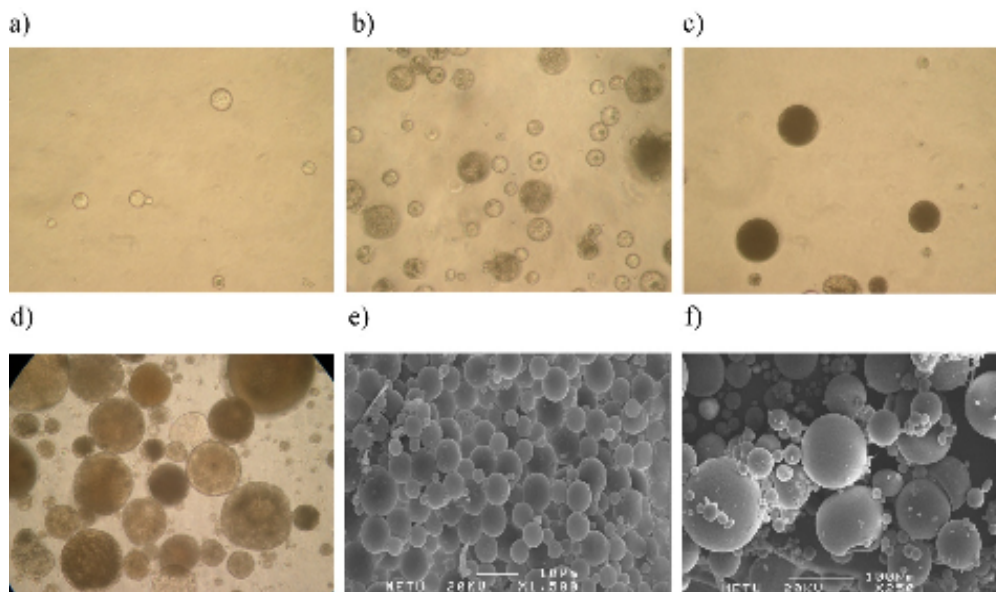


**Figure 17 - Morphology of DE microparticles.** Light microscope images; a) 10 mg/ml PLGA, b) 30 mg/ml PLGA, c) 75 mg/ml PLGA, d) 100 mg/ml PLGA under 40X magnification. SEM images; e) 10 mg/ml PLGA, b) 75 mg/ml PLGA in the organic phase respectively

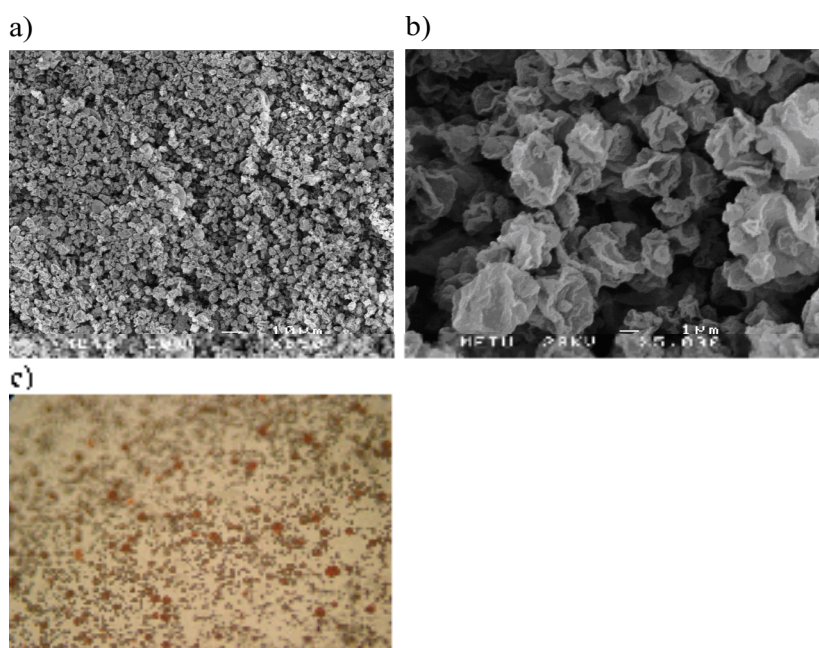


**Figure 18 - SEM images of doxorubicin loaded SE microparticles.** SEM images under (a) 550X and (b) 5000X. Figure c; light microscope image of SE particles (8 mg/ml PLGA) under 40X magnification

When two fabrication methods were compared the most profound difference was among their sizes and surface properties. SE particles looked much smaller than DE particles. However there were very small DE particles as well. Comparison of size was also done by dynamic light scattering but it did not revealed such a big difference.

SE particles looked red due to encapsulated doxorubicin while DE particles looked slightly pinkish. This is an expected scene, since SE particles contain more drug than DE particles.

A more detailed examination is done with SEM. DE particles all exhibited perfectly spherical shapes and smooth surfaces. There was pore formation to a very little extent. There is very low affinity between PLGA solvent chloroform and non solvent water. This causes slow polymer precipitation. Slow precipitation is known to cause non porous dense particles with low initial release rate [107]. The particles made by using SE method, however, were less spherical, showed wrinkly surfaces. Moreover, the particle shape was not well defined. Microparticles appearing as deflated balls might have resulted from lyophilization. During lyophilization the internal aqueous phase evaporates and the capsules can collapse.

### **3.6 Doxorubicin Release from Microparticles**

In vitro release of doxorubicin from PLGA microparticles was followed over 40 days. The release profiles from two different microparticle formulations were determined by reading the absorbance of released drug in phosphate buffer (PBS: 0.01 M, pH 7.4, 1ml) by using Elisa Reader at 480 nm. To measure Dox in PBS a new calibration curve was prepared. Figure 18 shows the standard curve of doxorubicin in PBS.

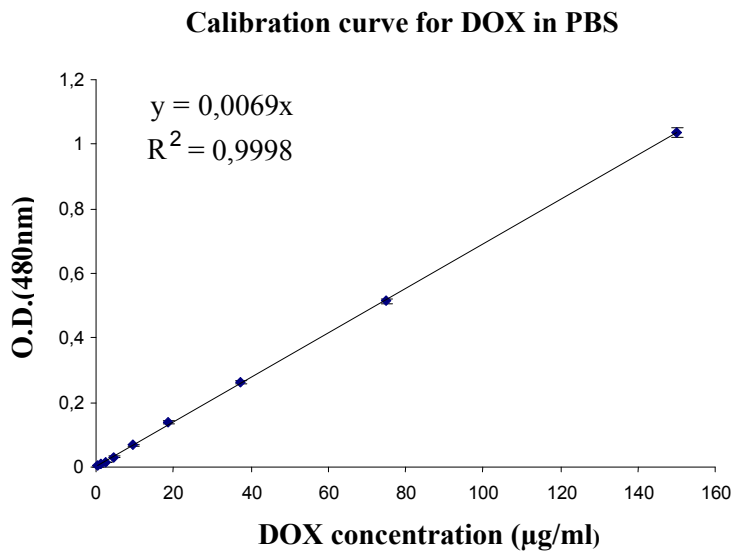


**Figure 19 - Calibration curve of doxorubicin in PBS**

This standard curve had a different slope than the one prepared by dissolving the drug in DMSO and using a different spectrophotometer. Because the absorbance values depend on the solvent in which drug is dissolved and the equipment used to measure the absorbance.

This calibration curve was used to determine the concentration of the drug in the release medium. Figure 19 shows the released drug from SE and DE particles over a period of 40 days.

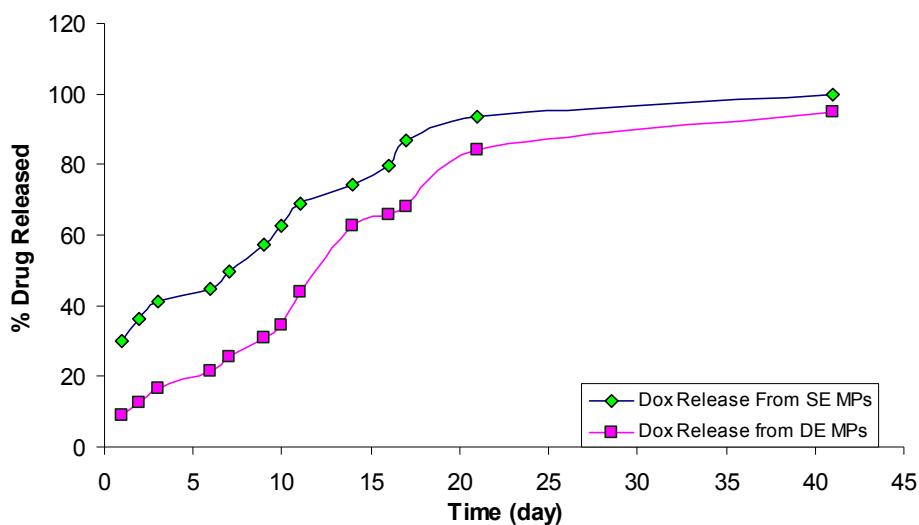


**Figure 20 - Release profile of doxorubicin from microparticles**

Figure shows Dox release from DE and SE methods into phosphate saline buffer pH 7.4 at 37°C. Both of the batches contain microparticles that encapsulate same amount of drug inside.

For release experiment particles were prepared by both of the methods setting the parameters that gave highest EE in previous experiments. On day 1, the Dox microparticles prepared by SE method released (30± 2.5) % of their total amount of encapsulated drug and the microparticles prepared by DE method released (3.6 ± 0.2). About 50% of the doxorubicin was released by SE microspheres on day 7 (49.89 ± 0.3) and by day 13 from the DE constructs. For about 93.4 ± 0.3% was released by day 21 from SE microspheres and 95.0± 3.2% by day 41 from DE constructs.

A closer look at the release profiles of both of the microspheres suggests the existence of three distinctive zones, namely the first 3 days, 3-17 days and 17–40 days. As it can be seen in the first 3 days there was an initial burst of 45% of drug

from microparticles prepared by SE method. On the other hand the initial burst was less (approximately 22%) for microparticles prepared by DE method.

When the experimental data from the first 3 days were fitted into a graph by least squares regression it was found that a linear line represented the data best. According to the graph, slope (release rate) of SE particles was 5.62 while DE particles were 3.74. The initial release rate of drug from SE particles was faster.

The release profiles demonstrate that the two batches presented a sustained release during the studied period. The burst effect can be attributed to the release of drug present within the cavities over the surface of the polymer and drug entrapped close to the surface. After the first 3 days release slowed down suggesting a depletion of Dox from within the available diffusion distance from the surface. During this second phase doxorubicin from the inner layers of the microparticles were released. This implies that most of the drug was distributed in the internal matrix of the polymer instead of near the surface.

As water imbibitions into the system increased, more ester bonds were cleaved and polymer chains cleave increased. As more of the polymer was degraded more cracks must had been formed. Water leakage from the cracks into the system increases in such a case so more polymer would come in contact with water and degraded. It is important to consider the dependency of deprecation rate on porosity as well.

The release rate of Dox from SE particles was significantly higher than DE particles. This can be explained by the phenomenon that SE particles' surface was wrinkled so a larger area came in contact with water which increased the drug diffusion to the release medium. Some literature findings show the opposite behavior. F. Tewes *et. al.* (2007) showed that during the first hours of release DE particles released more drug than SE particles. They tried to explain this effect by stating that the superficial layers of nanoparticles formulated by SE were less enriched in doxorubicin than

those formulated by DE. However their particles were very similar in surface characteristics. The higher drug loading might be responsible for higher release. In general, the release increases with increasing loading in the case of water soluble drugs (Ravivarapu et al., 2000; Bodmeier and McGinity, 1987; Bodmer *et. al.*, 1992).

In general, drug release from polymeric drug delivery systems is governed by diffusion process within the system and degradation characteristics of the polymer used. Rate is also influenced by the environment to which the system is exposed. The kinetics of drug release from a system can be modified to follow one of the several commonly known equations, such as first-order (i.e. square root of time) and zero-order (i.e., constant delivery) [92]. One way to find release rate is to put experimental release data into a graph than find the best fitting curve by comparing  $r^2$  values.

PLGA undergoes a hydrolysis process that occurs throughout the bulk of the material. The permeability changes with time as the polymer underwent bulk erosion, thus rendering the drug release rate somewhat unpredictable.

Release can be modified with some other ways as well. Increasing the mole of glycolide in the co-polymer increases its rate of biodegradation. In this study 75:25 ratio of lactide/glycolide was used. 50:50 ratio will degrade more rapidly. If polymers with same lactide/glycolide molar ratio polymer with lowest molecular mass degrade most rapidly.

There are some more accurate methods to study release kinetics. First of all sink conditions must be provided. To have sink conditions, large release volumes usually have to be used, thus impeding the drug concentrations required for the quantitative determinations. In this study release medium volume was kept low for making it possible to determine drug concentration by spectrophotometer. This would in turn disrupt sink conditions which is required for healthy assessment of drug release



kinetics. Besides, PLGA microparticles prepared in this study have high polydispersity index. This obligates to subdivide the continuous particle size distribution into N classes, each one comprehending particles showing the same diameter. This in turn requires the simultaneous solution of proper mass transport equations for each class as, in principle, drug release from each particles class is influenced by the presence of the other classes. Obviously, this reflects in a much more complex solution technique to be adopted. There are several mathematical models describing drug release from spherical devices (i.e. Koimumi and Panomsuk prepared a model describing drug release from non-erodible spherical devices) in the literature. A proper mathematical method has to be chosen by considering drug delivery systems' properties and putting related constants (such as diffusion coefficient of drug within the system, solubility of the drug within the system and degradation rate constant of the polymer) into the equation. For the implementation of the mathematical model a programming language (C++) can be used. More advance techniques involves using Monte Carlo simulations.

### **3.7 Cell Proliferation Assay on PLGA Microparticles**

XTT Cell Viability Assay was used to determine the rate of cell proliferation and to screen cytotoxic effects of empty and doxorubicin loaded PLGA microparticles.

Due to cell culture limitation it was not possible to study the long term effects of drug loaded particles on cells. So short-term cytotoxicity of microparticles on MCF-7 breast cancer cells was determined by using XTT assay. Figure 20 shows MCF-7 cell viability after 72h of incubation with microparticles prepared by single emulsion solvent evaporation method (SE-Dox-MPs) between 0.003 mg/ml to 1.66 mg/ml (maximum concentration equals to 150  $\mu$ M doxorubicin). Under the same conditions empty PLGA microparticles were also applied to the cells as the control group. Results in the figure represent Mean $\pm$  SEM. All experiments were carried out in triplicates.

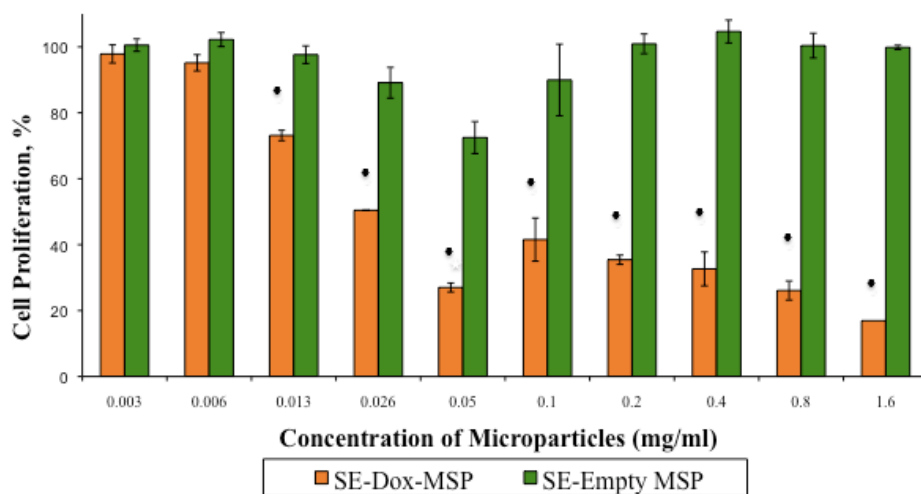


**Figure 21 - MCF-7 cell proliferation profiles after incubation with SE particles**

Cell proliferation was determined by XTT assay after 72 h. All experiments were carried out in triplicates. \* $p < 0.05$  relative to empty particles treated cells

One straight forward conclusion that can be driven from the cytotoxicity profile of microparticles is that Dox released from the microspheres prepared by single emulsion solvent evaporation method caused cell killing. This indicated that the bioactivity of the released Dox was unaffected by the encapsulation process which involves dissolving the drug in an organic solvent, sonication and lyophilization.

Toxicity profile of SE-Dox-MPs suggested that concentration amounts less than 0.006 mg/ml caused a mild toxicity. Concentrations at 1.66 mg/ml killed almost %15 of all MCF-7 cells in the cell culture. To characterize the drug cytotoxicity the inhibition concentration ( $IC_{50}$ ) was used. It is given as the concentration of the drug concentration at which 50% cells stop metabolizing. After 72 h of incubation,  $IC_{50}$  was determined as 0.095 mg/ml. This indicates the active release of doxorubicin is enough to elucidate cell killing effect even with very low dosages of particles.

Dox loaded microparticles prepared by double emulsion solvent evaporation method (DE-Dox-MPs) were applied to MCF-7 cells in order to see the toxicity profile. Figure 21 shows MCF-7 cell viability after 72 h of incubation with dosages between 40 mg/ml (containing 150  $\mu$ M doxorubicin) to 0.312 mg/ml (containing 0.5  $\mu$ M doxorubicin) DE-Dox-MPs.

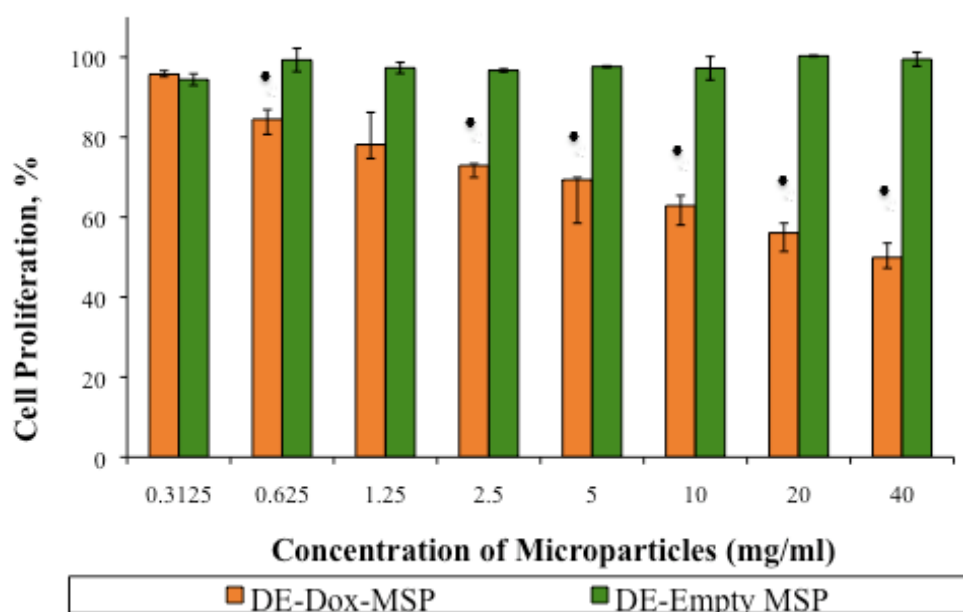


**Figure 22 - MCF-7 cell proliferation profiles after incubation with DE particles**  
Cell proliferation was determined by XTT assay after 72h. All experiments were carried out in triplicates. \* $p < 0.05$  relative to empty particles treated cells

When compared to SE microparticles, much more DE particles were added to have 150  $\mu$ M doxorubicin. That is due to their low drug loading. After 72h of incubation,  $IC_{50}$  was determined as 30 mg/ml.  $IC_{50}$  for SE particles was 0.095 mg/ml. This means that 0.095 mg/ml of SE particles have the same cell killing effect as 30 mg/ml DE particles.

No cytotoxicity of the empty PLGA microparticles was observed after 72 hours on MCF-7 cell line. This was an expected result because PLGA is biocompatible and neither it nor its degradation products cause toxic effects to cells. During the fabrication of microparticles organic solvent was used which is toxic. Since empty particles were not harmful to cells this indicates solvent evaporation step was successful. Majority of chloroform should have been evaporated.

### **3.8 Internalization of Doxorubicin Released from Microparticles**

Flourescence microscopy analysis results are given in figure 22 and 23. MCF -7 cells incubated with free doxorubicin showed the drug both in the prephery and cytoplasm. When drug is applied by means of microparticles it was observed that drug accumulation on the cell membrane increased. This might be the result of interactions of nanoparticles with the cell surface. This effect might aid internalization of the drug.

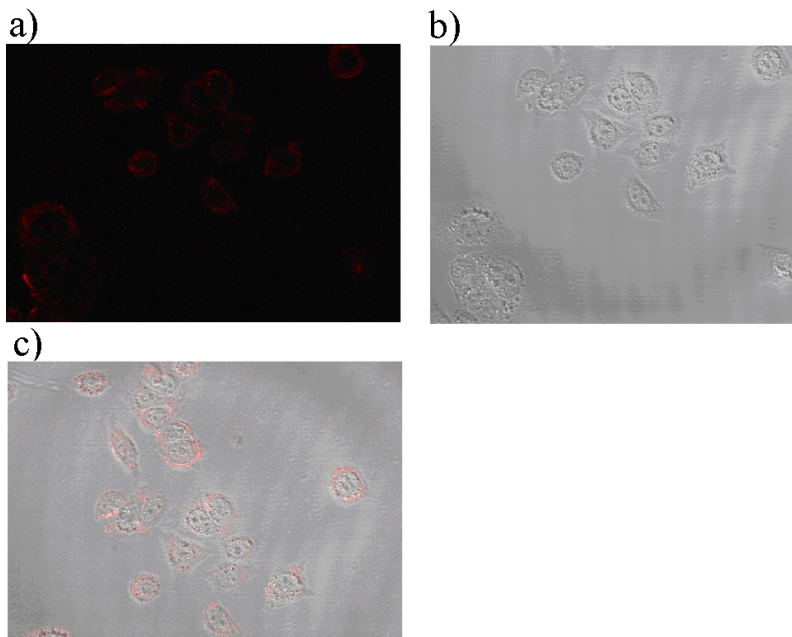


**Figure 23 - Confocal microscopy analysis MCF -7 incubated with free doxorubicin, a, fluorescence image; b, light microscope image; c, superimposed image of a and b**

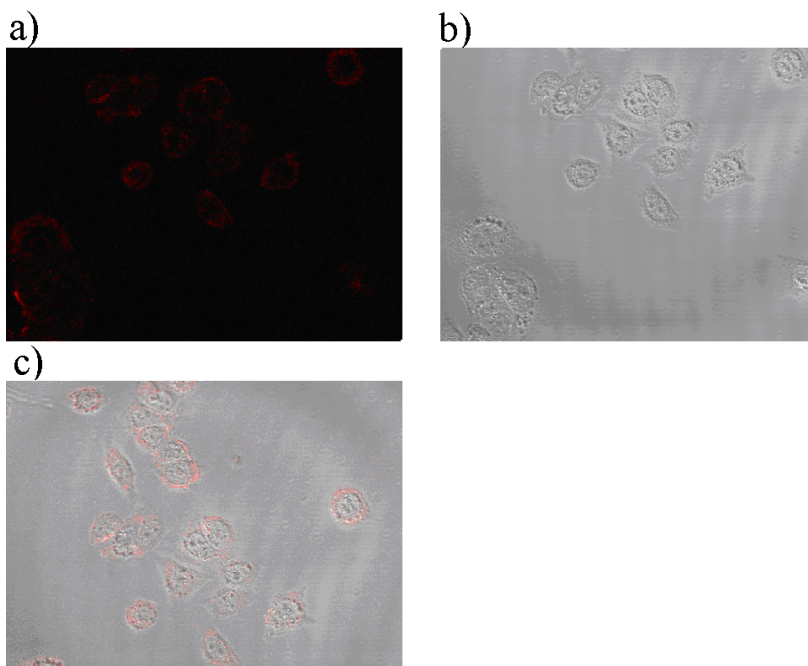


**Figure 24 - Confocal microscopy analysis MCF -7 incubated with doxorubicin loaded SE microparticles, a, fluorescence image; b, light microscope image; c, superimposed image of a and b**

### **3.9 Dox-TAT Conjugation Reaction with SMCC**

Doxorubicin was conjugated to TAT peptides by using SMCC as the cross-linker. SMCC contains amine reactive N-hydroxysuccinimide (NSH-ester) end and sulfhydryl reactive maleimide group. Maleimide has greater stability in aqueous environments than the NSH ester end. So first NSH-ester was reacted with the amine group on doxorubicin molecule. Second reaction was the conjugation of TAT to activated Dox.

#### **3.9.1 Activation of Doxorubicin**

This reaction contains 3 M equivalent of SMCC with respect to doxorubicin. Normally 40-80 fold molar excess is appropriate. Usually after the first reaction excess reagents are removed. Because crosslinker molecules which were not entered into the reaction will be competing for the thiols once there were added. However, the excess SMCC cannot be removed after the first reaction. Due to the very small and similar sizes of products and reactants a purification step was not possible. So the maleimide content contributed from the contaminating reacted cross linker may prevent subsequent conjugate formation. To overcome this SMCC concentration kept at minimum. Some of the TAT peptides was compromised. In order to compensate for this loss 3 times more TAT was added into the reaction in the second step. This reaction resulted in the formation of an amide bond between the drug and the cross-linker and formation of a reactive maleimide group. Reaction was followed by thin layer chromatography and the result is shown in Figure 25. First dot appeared where the initial reaction mixture was applied. Since Dox is colored on its own no special technique was needed for visualization. The first dot belongs to Dox. 2 hours after the reaction a new sample was applied next to the first. Another dot was appeared further away than the first one. This proves the reaction was successful. These introduced maleimide groups are stable for several days at 4°C. It is reported that

only 4% of them will decompose at neutral pH within 2 h at 30°C (Ishikawa et al., 1983).

### 3.9.2 Quantification of Sulphydryl Groups on TAT peptide

Free -SH groups on both of the peptides were quantified by the DTNB method. TAT was dissolved in water to have 19 mg/ml final concentration. 2  $\mu$ l from this stock solution was analyzed and moles of sulphydryl in the assay solution were calculated. Calculations were performed as shown below;

$$A_1(412 \text{ nm})=0.044$$

$$A_2(412 \text{ nm})=0.045$$

$$A_3(412 \text{ nm})=0.043$$

$$A_{\text{avr}}(412 \text{ nm})= 0.044$$

$$c = A / (bE)$$

where A(absorbance)=0.044, b(path length in centimeters)=1, c(concentration in M) E(Molar absorptivity)= 14,150  $\text{M}^{-1}\text{cm}^{-1}$ . Assay solution was 2.8 ml in all experiments.

The concentration in the spectrophotometric cuvette was calculated from the formula:

$$C = A / (bE)$$

$$C = \frac{0.044}{1 (14.150)} = 3.1 * 10^{-6} M$$

$$2.8 \text{ mL} \frac{1L}{1000\text{mL}} 3.1 * \frac{10^{-6} \text{ moles}}{L} = 8.68 * 10^{-9} \text{ moles}$$

$$\frac{8.68 * 10^{-9} \text{ moles}}{2 \mu\text{L}} * \frac{1\,000\,000 \mu\text{L}}{L} = 4.34 * 10^{-3} M = 0.0043 M$$

19 mg/ml TAT stock solution contains 0.0043 M –SH groups. However, theoretically this stock solution is 0.0103 M. There is one cysteine per one molecule of peptide. So –SH concentration should be 0.0103 M as well. Experimental value was 2.4 times less than the theoretical value.

Results indicate that 45% of all SH groups of TAT initially present were oxidized to form S-S bonds. In conjugation reaction maleimide end of the crosslinker only reacts with reduced cysteine residues (free thiols) on TAT peptides. If they are not in their free form this reaction will not occur and most of the peptide will be compromised. The possibility of degradation of peptide was also considered but the absorptions of stock peptide solutions at 215 nm were not significantly different that working solutions of peptides, which excluded this possibility. In order to restore the SH groups reduction with borohydride was performed.

### 3.9.3 Reduction of Sulfhydryl Groups on TAT Peptide

In order to determine optimum conditions for TAT peptide reduction, reaction was performed for 90 minutes and aliquots were taken at predetermined time points to analyze with DNTB method. Figure 24 the change in absorption as the reaction proceeds.



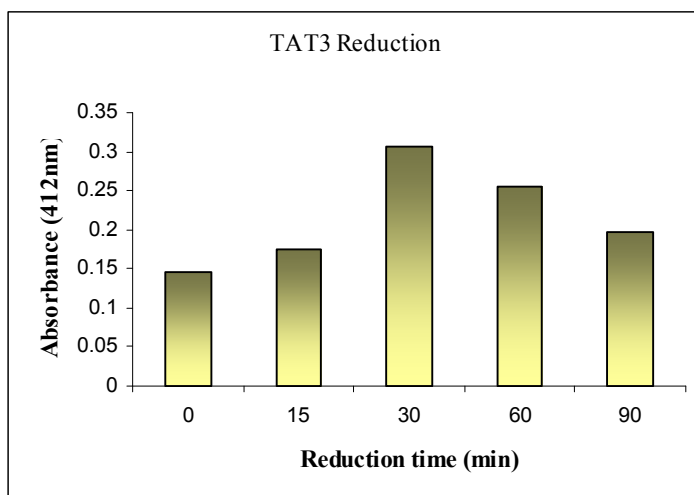


**Figure 25 - Re-formation of sulfhydryl groups on TAT**

Absorbance increase corresponds to the increase in free –SH groups. As it is seen from the graph 30 minutes was enough for -SH reduction. Reduction at longer times is not effective as re-oxidation occurred. Before all of the conjugation reactions performed TAT peptides were reduced for 30 minutes then used immediately for the conjugation reaction.

Sulfhydryl groups of terminal cysteine residues are readily oxidized and form disulfide bonds when the lyophilized peptides are reconstructed. When the free sulfhydryl groups are oxidized, SMCC conjugation reaction involving free thiols will be impaired. Since oxidation occurs any time during storage and handling it is impossible to fully prevent and it is very important to restore the free sulfhydryl groups before starting any reaction even if the cysteine residues are supposedly free. Reduction with sodium borohydride ( $\text{NaBH}_4$ ) is the most suitable method, for reducing the oxidized sulfhydryls for future use in cross-linking reactions. The biggest advantage is that it does not require an additional purification step. The excessive  $\text{NaBH}_4$  can be eliminated by acidification. The  $\text{NaBH}_4$  is hydrolyzed to

give  $\text{NaH}_2\text{BO}_3$  and  $\text{H}_2$  gas. Afterwards the reduced peptide can be used directly for the coupling reactions.

### 3.9.4 TAT Conjugation to Activated Doxorubicin

After 30 minutes of reduction TAT peptides were added to activated doxorubicin. Conjugation reaction was followed by TLC. Free doxorubicin, doxorubicin activation reaction mixture and TAT conjugation reaction mixture were spotted respectively at first second and third dots apart the start line. TLC paper is shown in Figure 25.



**Figure 26 - Thin layer chromatography of conjugation reaction products**

First spot on TLC paper belongs to doxorubicin before SMCC was added to the solution. Second spot belongs to the sample taken just before TAT addition to reaction mixture. Third spot is the final reaction product.

As it is seen from the figures free doxorubicin before the reaction is compared with the product (Dox-maleimide) at the end of the first reaction and with the final product at the end of the second reaction. Retention Factor ( $R_f$ ) calculations are shown below:

TAT-Dox Plate:

$R_f(\text{Dox})=0,14$

$R_f(\text{Dox-maleimide})=0,71$

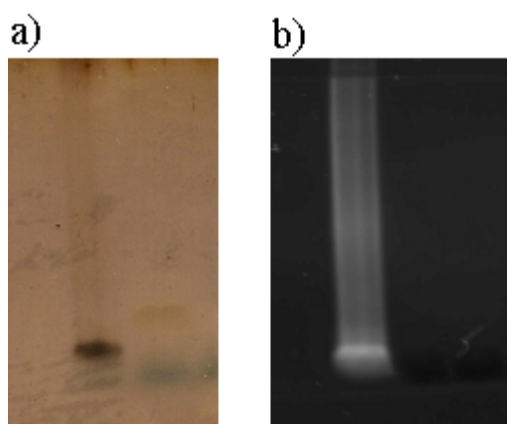
$R_f(\text{Dox-TAT})=0,54$

The significant change in  $R_f$  values indicates that the activation and conjugation reactions were successful. Another important point is that, in the subsequent steps of the reaction no more free drug was observed on TLC. Also after the second step no more maleimide conjugated Dox was visible. This proves that most of the free doxorubicin was maleimide conjugated and most of the activated Dox was conjugated to TAT.

Thin-layer chromatography is a commonly used technique in synthetic chemistry for identifying compounds, and following the progress of a reaction. It is a rapid, simple, and inexpensive method. The  $R_f$  depends on solvent system, absorbent (grain size, water content, and thickness), amount of material spotted and temperature. Hence it will be different for same compounds on different plates. So these were relative values and must be compared with the reference material (Doxorubicin) on the same plate under the same conditions. If  $R_f$  values of two compounds are the same they might be the same. If  $R_f$  values are different the two compounds are definitely different.

### 3.10 Visualization of Dox-Tat Conjugate on Tris-Tricine SDS-PAGE

The molecular weight of TAT was around 1700Da and doxorubicin was 580Da. Dox-TAT conjugation will be slightly higher than TAT peptide, which would be very difficult, if not impossible, to separate from each other by SDS-polyacrylamide gel electrophoresis (SDS-PAGE) assay. Since doxorubicin is a fluorescent compound, the ultraviolet image of the same SDS-PAGE gel was generated. Figure 26 shows Dox and TAT on SDS-PAGE. After silver staining both of the molecules became visible. The molecular weight of one band was around 600Da and the other was around 1700Da. First band belongs to Dox and the second one belongs to TAT. Dox was illuminated under UV light whereas TAT was not visible. With the help of this property Dox-TAT conjugate can be verified once it was subjected to SDS-PAGE assay.



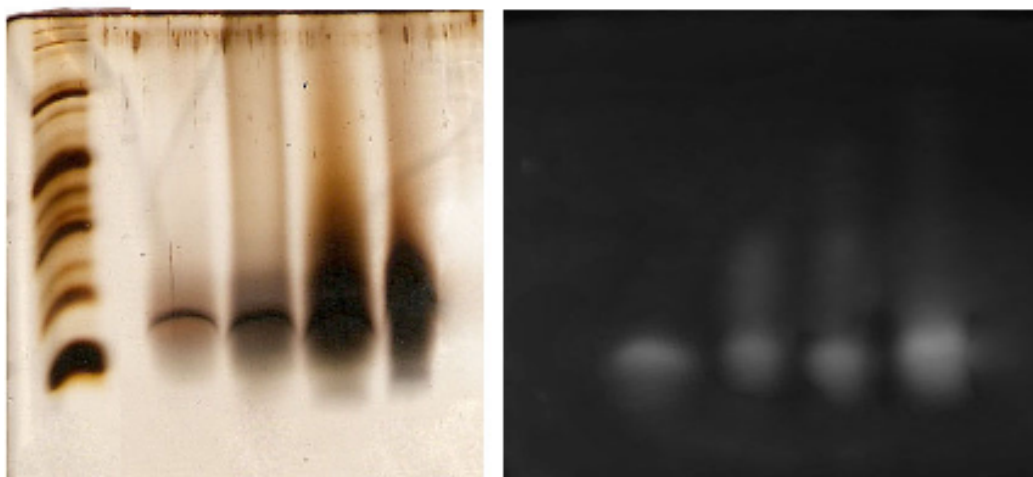
**Figure 27 - SDS-PAGE image of Dox and TAT**

Figure a, under visible light; b, under UV light

Figure 26 also shows that Dox moves just above the coomassie dye which is around 800 g/mol. TAT was larger than both so its band was observed at a higher level.

### 3.11 Purification of Dox-TAT Conjugate

To remove small molecules; unreacted Dox, SMCC and TEA from Dox-TAT conjugate were dialyzed. Samples were removed inside the tubing at pre determined time intervals (0, 6, 12, and 24 hours) and saved for later use in SDS-PAGE assay. After overnight purification all the samples were run at Tris Tricine SDS-PAGE gel and after silver staining below image was generated.



**Figure 28 - Reaction Products on SDS-PAGE Gel**

Samples inside the dialysis bag were removed at  $t=0$ ,  $t=6$ ,  $t=12$ ,  $t=24$  hours. Bands on the gel correspond to these samples respectively. First band is the marker having 1.5 kDa band at the bottom and 3 kDa band on top of it. Image at the left shows actual gel after silver staining. Image at the right shows UV image of the gel.

Bands respectively belong to reaction product after before dialysis, product after 6 hours of dialysis, product after 12 hours of dialysis, product after 24 hours of dialysis. The smear belongs to free drug that was not conjugated. As dialysis continues free drug increases, however it does not go out of the tubing. This result shows that initially there was some free drug but it was not that much. As dialysis

continues bonds between Dox and TAT were cleaved. So conjugate was not stable over long periods of time in PBS, pH 7.0. It has to be stored in its lyophilized form.

### 3.12 Cell Growth Inhibition of Dox-TAT Conjugate

Figure 28 shows 600 nM resistant MCF-7 cell viability after 72h of incubation with Dox-TAT chemical conjugation and free Dox.

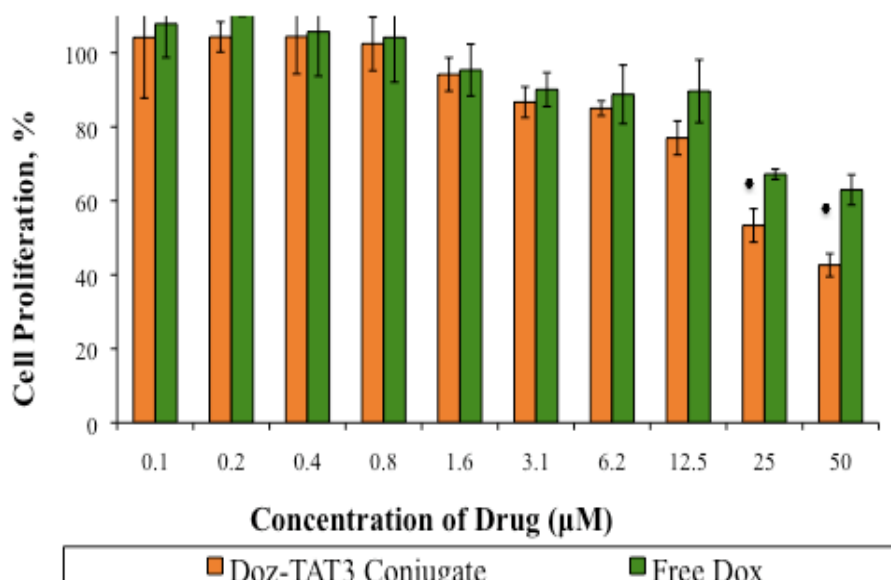


**Figure 29 - Cell proliferation profiles of 600nm Dox resistant MCF-7 cell line after 72h incubation with Dox-TAT conjugate and free Dox**

Even though microparticles were once hoped to overcome MDR (Barraud et al., 2005, Batrakova et al., 1996, Lee et al., 2005, Rapoport et al., 2002, Sahoo and Labhasetwar, 2005) some recent research failed to prove it. It is shown that P-gp substrates, such as doxorubicin and paclitaxel, delivered to MDR cells by PLGA nanoparticles, are still susceptible to efflux by P-gp [93]. For this reason in this study

a synthetic peptide with similarities to protein transduction domains are evaluated for its ability to carry doxorubicin, an important P-gp substrate, into resistant cells.

Cytotoxicity profiles of Dox-TAT conjugate and free Dox was similar at low drug concentrations. Only at higher concentrations (25-50  $\mu\text{M}$ ) Dox-TAT seems to be more potent. It was postulated that the thioether linkage is stable to reducing conditions of human serum for several hours [108]. That time might not been enough for the conjugate to enter into the cells and show its effect. The bond between Dox and TAT might have degraded during sample preparation and storage as well. Underlying mechanism needs further evaluation. Either TAT carried Dox inside the cell by its internalization ability or it facilitated drugs internalization into nucleolus with the help of its nuclear localization signal similar sequences. Some drawback on the system is lack of specificity and concern about causing the drug to loose its activity. The bond is not readily degradable in the endosomes so cytotoxicity of some conjugates might be reduced [108].

## 4 CHAPTER

### CONCLUSION

The purpose of this study was to develop doxorubicin delivery systems.

Two different microparticle fabrication methods were compared; double emulsion solvent evaporation (DE) and single emulsion solvent evaporation (SE) method for encapsulation of doxorubicin into PLGA microparticles. The most appropriate method was the SE techniques which lead to higher encapsulation efficiencies. Processing factors were evaluated for their effects on encapsulation efficiency and results indicated that any change that hinders drug diffusion would result in increased drug content in microparticles.

Incorporation of Dox in PLGA microspheres can maintain local levels of the drug below the toxic level and above the minimum effective concentration. This would enhance the cytotoxicity in a more controlled manner compared to that of free drug and decrease the number of doses administered. Polymeric carrier systems are supposed to reduce Dox levels in the heart and decrease nonspecific organ toxicity and target the drug to the tumor site by enhanced extravasation across the leaky endothelium of solid tumors.

Promising results were obtained in delivery of doxorubicin into resistance cancer cells as well. When doxorubicin was chemically conjugated to a cell penetrating peptide, its effect was more obvious on resistant cancer cells when compared to that of free drug. In the future, once mechanism underlying this observation studied further, peptides might be alternative ways of overcoming MDR.



## REFERENCES

1. Bertram JS. The molecular biology of cancer. *Mol Aspects Med* 2000; 21:167-223
2. Hanahan, D. and R. A. Weinberg. "The hallmarks of cancer." *Cell* 100.1 (2000): 57-70
3. Franks, L. M., Teich, N. M., 2003. Introduction to the cellular and molecular biology of cancer, 3rd edition Oxford University Press, p125
4. Fidler, I. J. "Tumor heterogeneity and the biology of cancer invasion and metastasis." *Cancer Res.* 38.9 (1978): 2651-60
5. Jemal, A. et al. "Cancer statistics, 2008." *CA Cancer J.Clin.* 58.2 (2008): 71-96
6. American Cancer Society: Cancer Facts and Figures 2008. Atlanta, Ga: American Cancer Society, 2008
7. National Cancer Institute, SEER Cancer Statistics Review 1975-2005
8. Zimmerman, Barbara T. *Understanding Breast Cancer Genetics*. Jackson, MS, USA, University Press of Mississippi, 2004, *Nutritional Oncology* by David Heber, George L. Blackburn, Vay Liang W. Go, John Milner, Published by Academic Press, 2006
9. Antoniou, A. et al. "Average risks of breast and ovarian cancer associated with BRCA1 or BRCA2 mutations detected in case Series unselected for family history: a combined analysis of 22 studies." *Am.J.Hum.Genet.* 72.5 (2003): 1117-30.
10. King, M. C., J. H. Marks, and J. B. Mandell. "Breast and ovarian cancer risks due to inherited mutations in BRCA1 and BRCA2." *Science* 302.5645 (2003): 643-46
11. Narod, S. A. et al. "Tamoxifen and risk of contralateral breast cancer in BRCA1 and BRCA2 mutation carriers: a case-control study. Hereditary Breast Cancer Clinical Study Group." *Lancet* 356.9245 (2000): 1876-81.

12. Ford D, Easton DF, Bishop DT, Narod SA, Goldgar DE., Risks of cancer in BRCA1-mutation carriers. Breast Cancer Linkage Consortium, *Lancet*. 1994 Mar 19; 343(8899):692-5
13. Risch HA, McLaughlin JR, Cole DE, Rosen B, Bradley L, Kwan E, Jack E, Vesprini DJ, Kuperstein G, Abrahamson JL, Fan I, Wong B, Narod SA., Prevalence and penetrance of germline BRCA1 and BRCA2 mutations in a population series of 649 women with ovarian cancer, *Am J Hum Genet*. 2001 Mar; 68(3):700-10
14. Bartek J, Falck J, Lukas J.,CHK2 kinase--a busy messenger, *Nat Rev Mol Cell Biol*. 2001 Dec;2(12):877-86. Review
15. Meijers-Heijboer H, van den Ouweland A, Klijn J, Wasielewski M, de Snoo A, Oldenburg R, Hollestelle A, Houben M, Crepin E, van Veghel-Plandsoen M, Elstrodt F, van Duijn C, Bartels C, Meijers C, Schutte M, McGuffog L, Thompson D, Easton D, Sodha N, Seal S, Barfoot R, Mangion J, Chang-Claude J, Eccles D, Eeles R, Evans DG, Houlston R, Murday V, Narod S, Peretz T, Peto J, Phelan C, Zhang HX, Szabo C, Devilee P, Goldgar D, Futreal PA, Nathanson KL, Weber B, Rahman N, Stratton MR; CHEK2-Breast Cancer Consortium., Low-penetrance susceptibility to breast cancer due to CHEK2(\*)1100delC in noncarriers of BRCA1 or BRCA2 mutations, *Nat Genet*. 2002 May; 31(1):55-9. Epub 2002 Apr 22."
16. Vahteristo P, Bartkova J, Eerola H, Syrjäkoski K, Ojala S, Kilpivaara O, Tamminen A, Kononen J, Aittomäki K, Heikkilä P, Holli K, Blomqvist C, Bartek J, Kallioniemi OP, Nevanlinna H.,A CHEK2 genetic variant contributing to a substantial fraction of familial breast cancer., *Am J Hum Genet*. 2002 Aug; 71(2):432-8. Epub 2002 Jul 28
17. Easton, D., D. Ford, and J. Peto. "Inherited susceptibility to breast cancer." *Cancer Surv*. 18 (1993): 95-113
18. Anthony S. Fauci, Eugene Braunwald, Dennis L. Kasper, Stephen L. Hauser, Dan L. Longo, J. Larry Jameson, and Joseph Loscalzo, Harrison's

Principles of Internal Medicine, University of California Press, 2000, 17th Edition, p35

19. Cancer Explained, Professor Fred Stephens, Wakefield Press
20. Guy B. Faguet, The War on Cancer: An Anatomy of Failure, a Blueprint for the Future, Springer, 2005
21. Weiss RB, The anthracyclines: will we ever find a better doxorubicin?, *Semin. Oncol.* 19 (6): 670–86., 1992
22. Williams Hematology, 7th Edition Marshall A. Lichtman, Ernest Beutler, Thomas J. Kipps, Uri Seligsohn, Kenneth Kaushansky, Josef T. Prechal
23. Doxorubicin Proposed PI Update Final Approved Label - May 8, 2003
24. Gewirtz, D. A. "A critical evaluation of the mechanisms of action proposed for the antitumor effects of the anthracycline antibiotics adriamycin and daunorubicin." *Biochem.Pharmacol.* 57.7 (1999): 727-41.
25. Minotti, G. et al. "Anthracyclines: molecular advances and pharmacologic developments in antitumor activity and cardiotoxicity." *Pharmacol.Rev.* 56.2 (2004): 185-229
26. K. Dano, S. Frederiksen and P. Hellung-Larsen, Inhibition of DNA and RNA synthesis by daunorubicin in sensitive and resistant Ehrlich ascites tumor cells in vitro. *Cancer Res* 32 (1972), pp. 1307–1314,
27. W.D. Meriwether and N.R. Bachur, Inhibition of DNA and RNA metabolism by daunorubicin and adriamycin in L1210 mouse leukemia. *Cancer Res* 32 (1972), pp. 1137–1142
28. J.J. Wang, D.S. Chervinsky and J.M. Rosen, Comparative biochemical studies of adriamycin and daunomycin in leukemic cells. *Cancer Res* 32 (1972), pp. 511–515
29. F.A. Fornari, Jr, W.D. Jarvis, S. Grant, M.S. Orr, J.K. Randolph, F.K.H. White, V.R. Mumaw, E.T. Lovings, R.H. Freeman and D.A. Gewirtz, Induction of differentiation and growth arrest associated with nascent (nonoligosomal) DNA fragmentation and reduced c-myc expression in MCF-7

- human breast tumor cells after continuous exposure to a sublethal concentration of doxorubicin. *Cell Growth Differ* 5 (1994), pp. 723–733
30. Singal PK, Deally CM, Weinberg LE. Subcellular effects of adriamycin in the heart: a concise review. *J Mol Cell Cardiol* 1987; 19:817–28.
  31. Bertram G. Katzung, Basic & Clinical Pharmacology, 10th Edition, Academic Press, 2002, pp. 138
  32. Ambudkar, S. V. et al. "Biochemical, cellular, and pharmacological aspects of the multidrug transporter." *Annu. Rev. Pharmacol. Toxicol.* 39 (1999): 361-98
  33. Gille L, Nohl H. Analyses of the molecular mechanism of adriamycin-induced cardiotoxicity. *Free Radic Biol Med* 1997; 23: 775-82
  34. Takemura G, Fujiwara H. Doxorubicin-induced cardiomyopathy from the cardiotoxic mechanisms to management. *Prog Cardiovasc Dis* 2007; 49:330–52.
  35. Doroshow JH., Anthracycline antibiotic-stimulated superoxide, hydrogen peroxide, and hydroxyl radical production by NADH dehydrogenase. *Cancer Res* 1983; 43:4543–51
  36. Davies KJ, Doroshow JH. Redox cycling of anthracyclines by cardiac mitochondria. I. Anthracycline radical formation by NADH dehydrogenase. *J Biol Chem* 1986; 261:3060–7.
  37. B. Kalyanaraman, J. Joseph and S. Kalivendi et al., Doxorubicin-induced apoptosis: Implications in cardiotoxicity, *Mol. Cell Biochem.* 234-235 (2002), pp. 119–124.
  38. S.M. Swain, F.S. Whaley and M.S. Ewer, Congestive heart failure in patients treated with doxorubicin: A retrospective analysis of three trials, *Cancer* 97 (2003), pp. 2869–2879
  39. Joguparthi, V. and B. D. Anderson. "Liposomal delivery of hydrophobic weak acids: enhancement of drug retention using a high intraliposomal pH." *J.Pharm.Sci.* 97.1 (2008): 433-54.

40. Choudhury, P. K., C. S. Chauhan, and M. S. Ranawat. "Osmotic delivery of flurbiprofen through controlled porosity asymmetric membrane capsule." *Drug Dev.Ind.Pharm.* 33.10 (2007): 1135-41.
41. Trickler, W. J., A. A. Nagvekar, and A. K. Dash. "A novel nanoparticle formulation for sustained paclitaxel delivery." *AAPS.PharmSciTech.* 9.2 (2008): 486-93.
42. Yang, T. et al. "Liposome formulation of paclitaxel with enhanced solubility and stability." *Drug Deliv.* 14.5 (2007): 301-08
43. T.M. Allen, P.R. Cullis, *Drug Delivery Systems: Entering the Mainstream Science* 303 2004 1818-1822
44. Waterhouse DN, Tardi PG, Mayer LD, Bally MB.,A comparison of liposomal formulations of doxorubicin with drug administered in free form: changing toxicity profiles.*Drug Saf.* 2001; 24(12):903-20
45. Petsev, D. N. (Dimitar Nikolov), *Emulsions: structure, stability and interactions*, Elsevier, c2004
46. Narang, A.S., Delmarre, D., Gao, D., 2007. Stable drug encapsulation in micelles and microemulsions. *Int. J. Pharm.* 345, 9–25
47. Qingguo Xu, Alison Crossley, Jan Czernuszka, Preparation and characterization of negatively charged poly (lactic-co-glycolic acid) microspheres, *Journal of Pharmaceutical Sciences*, 2008
48. R. B. Merrifield (1963). "Solid Phase Peptide Synthesis. I. The Synthesis of a Tetrapeptide". *J. Am. Chem. Soc.* 85 (14): 2149–2154
49. T. Kimmerlin, D. Seebach, '100 years of peptide synthesis': ligation methods for peptide and protein synthesis with applications to beta-peptide assemblies.*J Pept Res.* 2005 Feb; 65(2):229-60.
50. Peptide Guide, *Solid Phase Peptide Synthesis*, Mayer, Telford Press, 2009, pp. 67
51. H. Weigmann, Reduction of disulfide bonds in keratin with 1, 4-dithiothreitol. I. Kinetic investigation, *Journal of Polymer Science Part A-1: Polymer Chemistry* 1968 6 (8), 2237-2253

52. Koken SE, Greijer AE, Verhoef K, van Wamel J, Bukrinskaya AG, Berkhout B, Intracellular analysis of in vitro modified HIV Tat protein, *J Biol Chem.* 1994 Mar 18;269(11):8366-75
53. McKillop AM, McCluskey JT, Boyd AC, Mooney MH, Flatt PR, O'Harte FPM: Production and characterization of specific antibodies for evaluation of glycated insulin in plasma and biological tissues. *J Endocrinol.* 167:1 53 –163, 2000
54. Burns, J. A., Butler, J. C., Moran, J., and M., W. G. (1991) Selective reduction of disulfides by tris (2-carboxyethyl) phosphine. *J. Org. Chem.* 56, 2648 –2650.
55. Getz, E. B., Xiao, M., Chakrabarty, T., Cooke, R., and Selvin, P. R. (1999) A comparison between the sulfhydryl reductants tris(2-carboxyethyl)phosphine and dithiothreitol for use in protein biochemistry. *Anal. Biochem.* 273, 73– 80.
56. Guo, N.-H., Krutzsch, H. C., Inman, J. K., Shannon, C. S., and Roberts, D. D. (1997) Antiproliferative and antitumor activities of D-reverse peptides derived from the second type-1 repeat of thrombospondin-1. *J. Peptide Res.* 50, 210 –220
57. Shafer DE, Inman JK, Lees; Reaction of Tris (2- carboxyethyl) phosphine (TCEP) with maleimide and alpha-haloacyl groups: anomalous elution of TCEP by gel filtration; *A. Anal. Biochem* 2000, 282, 161-164
58. Nagy L, Nagata M, Szabo S., Protein and non-protein sulfhydryls and disulfides in gastric mucosa and liver after gastrotoxic chemicals and sucralfate: possible new targets of pharmacologic agents., *World J Gastroenterol.* 2007 Apr 14; 13(14):2053-60.
59. Kress LF, Laskowski M Sr., The basic trypsin inhibitor of bovine pancreas. VII. Reduction with borohydride of disulfide bond linking half-cystine residues 14 and 38. *J Biol Chem.* 1967 Nov 10;242(21):4925-9.

60. Light A, Sinha NK. Difference in the chemical reactivity of the disulfide bonds of trypsin and chymotrypsin. *J Biol Chem.* 1967 Mar 25; 242(6):1358-9.
61. HIV Tat, its TARgets and the control of viral gene expression, Claudio Brigati, Mauro Giacca, Douglas M Noonan, Adriana Albini, *FEMS Microbiology Letters*, Volume 220 Issue 1 Page 57-65, March 2003
62. Transcellular protein transduction using the Tat protein of HIV-1, Antonio Fittipaldi and Mauro Giacc, *Advanced Drug Delivery Reviews* Volume 57, Issue 4, 28 February 2005, pp. 597-608
63. Tackling tat, Jonathan Karn, *Journal of Molecular Biology*, Volume 293, Issue 2, 22 October 1999, pp. 235-254
64. Tat-mediated delivery of heterologous proteins into cells, Fawell S, Seery J, Daikh Y, Moore C, Chen LL, Pepinsky B, Barsoum J; *Proc Natl Acad Sci U S A.* 1994 Jan 18;91(2):664-8.
65. Kalderon, D., B. L. Roberts, W. D. Richardson, and A. E. Smith. 1984. A short amino acid sequence able to specify nuclear location. *Cell* 39:499-509.
66. Kao, S. Y., A. F. Calman, P. A. Luciw, and B. M. Peterlin. 1987. Anti-termination of transcription within the long terminal repeat of HIV-1 by tat gene product. *Nature (London)* 330:489-493
67. Vivès E, Brodin P, Lebleu B., A truncated HIV-1 Tat protein basic domain rapidly translocates through the plasma membrane and accumulates in the cell nucleus. *J Biol Chem.* 1997 Jun 20;272(25):16010-7
68. Zhao M., Kircher M., Josephon L. (2002) Differential Conjugation of TAT Peptide to superparamagnetic nanoparticles and its effect on cellular uptake, *Bioconjugate Chem.*, 13, 840-844.
69. Antonio Fittipaldi, Mauro Giacca, *Advanced Drug Delivery Reviews*, Volume 57, Issue 4, 28 February 2005, pp.597-608

70. T. Suzuki, S. Futaki, M. Niwa, S. Tanaka, K. Ueda and Y. Sugiura, Possible existence of common internalization mechanisms among arginine-rich peptides, *J. Biol. Chem.* 277 (2002), pp. 2437–2443
71. Prochiantz, Homeodomain-derived peptides. In and out of the cells, *Ann. N.Y. Acad. Sci.* 886 (1999), pp. 172–179
72. E. Vives, J.P. Richard, C. Rispal and B. Lebleu, TAT peptide internalization: seeking the mechanism of entry, *Curr. Protein Pept. Sci.* 4 (2003), pp. 125–132
73. A. Ferrari, V. Pellegrini, C. Arcangeli, A. Fittipaldi, M. Giacca and F. Beltram, Caveolae-mediated internalization of extracellular HIV-1 Tat fusion proteins visualized in real time, *Molec. Ther.* 8 (2003), pp. 284–294
74. Christof M. Niemeyer, *Bioconjugation Protocols: Strategies and Methods (Methods in Molecular Biology)*, volume 283, Humana Press, 10 Jun 2004
75. Zanta MA, Belguise-Valladier P, Behr JP. Gene delivery: a single nuclear localization signal peptide is sufficient to carry DNA to the cell nucleus. *Proc. Natl Acad. Sci. USA* (1999) 96:91–96
76. Sandra Console, Cornelia Marty, Carlos García-Echeverría, Reto Schwendener, and Kurt Ballmer-Hofer, Antennapedia and HIV Transactivator of Transcription (TAT) "Protein Transduction Domains" Promote Endocytosis of High Molecular Weight Cargo upon Binding to Cell Surface Glycosaminoglycans, *J. Biol. Chem.*, Sep 2003; 278: 35109 - 35114.
77. C. Marty, C. Meylan, H. Schott, K. Ballmer-Hofer, and R. A. Schwendener. Enhanced heparan sulfate proteoglycan-mediated uptake of cell-penetrating peptide-modified liposomes. *Cell. Mol. Life Sci.* 61(14):1785–1794 (2004)
78. He, Liumin et al. "The influence of laminin-derived peptides conjugated to Lys-capped PLLA on neonatal mouse cerebellum C17.2 stem cells." *Biomaterials* 30.8 (2009): 1578-86



79. MR, Raucher D, Balu N, Michael Colvin O, Ludeman SM, Chilkoti A., Evaluation of an elastin-like polypeptide-doxorubicin conjugate for cancer therapy, *Dreher J Control Release*. 2003 Aug 28; 91(1-2):31-43
80. G. D. Lewis Phillips, G. Li, D. L. Dugger, L. M. Crocker, K. L. Parsons, E. Mai, W. A. Blattler, J. M. Lambert, R. V.J. Chari, R. J. Lutz, et al., Targeting HER2-Positive Breast Cancer with Trastuzumab-DM1, an Antibody-Cytotoxic Drug Conjugate, *Cancer Res.*, November 15, 2008; 68(22): 9280 - 9290
81. Temsamani and Vidal, 2004 J. Temsamani and P. Vidal, The use of cell-penetrating peptides for drug delivery, *Drug Discov. Today* 9 (2004), pp. 1012–1019
82. Luca Gianni, Eugene H. Herman, Steven E. Lipshultz, Giorgio Minotti, Narine Sarvazyan, Douglas B. Sawyer, Anthracycline Cardiotoxicity: From Bench to Bedside, *Journal of Clinical Oncology*, Vol 26, No 22 (August 1), 2008: pp. 3777-3784
83. Gabizon A, Catane R, Uziely B, Kaufman B, Safra T, Cohen R, Martin F, Huang A, Barenholz Y., Prolonged circulation time and enhanced accumulation in malignant exudates of doxorubicin encapsulated in polyethylene-glycol coated liposomes, *Cancer Res*. 1994 Feb 15;54(4):987-92
84. Emulsions: structure, stability and interactions, Petsev, D. N. (Dimitar Nikolov), Amsterdam; London: Elsevier, c2004
85. Ellman, G.L. (1959) Tissue sulfhydryl groups. *Arch. Biochem. Biophys.*82, 70-72
86. Collier HB (1973). "Letter: A note on the molar absorptivity of reduced Ellman's reagent, 3-carboxylato-4-nitrothiophenolate". *Anal. Biochem.* 56 (1): 310–1
87. Riddles, P.W., et al. (1983) Reassessment of Ellman's reagent. *Meth. Enzymol.*, 91, 49-
88. Hermanson, G. T. (1996) *Bioconjugate Techniques*, Academic Press, San Diego.

89. I. Brigger, C. Dubernet and P. Couvreur, Nanoparticles in cancer therapy and diagnosis. *Advanced Drug Delivery Reviews* 54 (2002), pp. 631–651
90. PLGA nanoparticles of different surface properties: preparation and evaluation of their body distribution. Esmaeili F, Ghahremani MH, Esmaeili B, Khoshayand MR, Atyabi F, Dinarvand R. *Int J Pharm.* 2008 Feb 12;349(1-2):249-55
91. Specific and non-specific phagocytosis of ligand-grafted PLGA microspheres by macrophages *European Journal of Pharmaceutical Sciences*, Volume 36, Issues 4-5, 2 March 2009, pp. 474-485
92. Transdermal and topical drug delivery systems by Tapash K. Ghosh, William R. Pfister, Su Il Yum, 1997, Interpharm Press, 348p
93. Susceptibility of nanoparticle-encapsulated paclitaxel to P-glycoprotein-mediated drug efflux, Mahesh D. Chavanpatil, Yogesh Patil and Jayanth Panyam, *International Journal of Pharmaceutics*, Volume 320, Issues 1-2, 31 August 2006, pp. 150-156
94. K. Elkharraz, N. Faisant, C. Guse, F. Siepmann, B. Arica-Yegin, J.M. Oger, R. Gust, A. Goepferich, J.P. Benoit and J. Siepmanna, Paclitaxel-loaded microparticles and implants for the treatment of brain cancer: Preparation and physicochemical characterization, *International Journal of Pharmaceutics*, Volume 314, Issue 2, 18 May 2006, pp. 127-136
95. Polylactide Microparticles Prepared by Double Emulsion/Evaporation Technique. I. Effect of Primary Emulsion Stability, Nicole Nihant, Chantal Schugens, Christian Grandfils, Robert Jérôme, Philippe Teyssié, *Pharmaceutical Research*, Volume 11, Number 10, October, 1994
96. Improvement of the encapsulation efficiency of oligonucleotide-containing biodegradable microspheres, Freytag T, Dashevsky A, Tillman L, Hardee GE, Bodmeier R., *J Control Release.* 2000 Oct 3; 69(1):197-207
97. Polymer-surfactant nanoparticles for sustained release of water-soluble drugs, Chavanpatil Mahesh D; Khadair Ayman; Patil Yogesh; Handa

- Hitesh; Mao Guangzhao; Panyam Jayanth, *Journal of pharmaceutical sciences* 2007; 96(12):3379-89.
98. Effect of WOW process parameters on morphology and burst release of FITC-dextran loaded PLGA microspheres, Shirui Mao, Jing Xu, Cuifang Cai, Oliver Germershaus, Andreas Schaperc, Thomas Kissel, *International Journal of Pharmaceutics*, Volume 334, Issues 1-2, 4 April 2007, pp. 137-148
99. T Painbeni, M.C Venier-Julienne and J.P Benoit, Internal morphology of poly(d,l-lactide-co-glycolide) BCNU-loaded microspheres. Influence on drug stability, *European Journal of Pharmaceutics and Biopharmaceutics*, Volume 45, Issue 1, January 1998, pp. 31-39
100. Formulation of Anastrozole Microparticles as Biodegradable Anticancer Drug Carriers, Zidan AS, Sammour OA, Hammad MA, Megrab NA, Hussain MD, Khan MA, Habib MJ., *AAPS PharmSciTech*. 2006; 7(3)
101. Wang D, Robinson DR, Kwon GS, Samuel J. Encapsulation of plasmid DNA in biodegradable poly(D,L-lactic-coglycolic acid) microspheres as a novel approach for immunogene delivery. *J Control Release*. 1999; 57:9-18
102. Budhian, S.J. Siegel and K.I. Winey, Haloperidol-loaded PLGA nanoparticles: Systematic study of particle size and drug content, *International Journal of Pharmaceutics*, Volume 336, Issue 2, 24 May 2007, pp. 367-375
103. Malvern Instruments Dynamic Light Scattering Technical Note (2008)
104. Kwon HY, Lee JY, Choi SW, Jang Y, Kim JH. Preparation of PLGA nanoparticles containing estrogen by emulsification-diffusion method. *Colloids Surf A: Physicochem Eng*.
105. Chorny M, Fishbein I, Danenberg HD, Golomb G. Lipophilic drug loaded nanospheres prepared by nanoprecipitation: effect of formulating variables on size, drug recovery and release kinetics. *J Control Release*. 2002;83:389-400
106. Quintanar-Guerrero D, Fessi H, Allémann E, Doelker E. Influence of stabilizing agents and preparative variables on the formation of poly(d,l-lactic

acid) nanoparticles by an emulsification-diffusion technique. *Int J Pharm.* 1996; 143:133-141

107. Xiaosong Luan, Marc Skupin, Jürgen Siepmann and Roland Bodmeier, Key parameters affecting the initial release (burst) and encapsulation efficiency of peptide-containing poly(lactide-co-glycolide) microparticles, *International Journal of Pharmaceutics*, Volume 324, Issue 2, 6 November 2006, pp.168-175

108. Frank J. Dixon, *Advances in Immunology*, Volume 56, Academic Press, 2002, pp 146

## APPENDIX A

### TRIS-TRICINE SDS-PAGE GEL BUFFERS

#### **3x Gel Buffer (3M Tris HCl, 0.3% SDS, pH 8.45)**

18.16 g Tris

4.16ml 37% HCl 12M (to have 1M in the end)

0,15g SDS

Fill up to 50 ml w/ H<sub>2</sub>O (add 30ml H<sub>2</sub>O first then add HCl the fill to 50ml)

#### **10X Cathode buffer (1M Tris, 1M Tricine, 0.1% SDS, pH 8.25)**

6,057 g Tris

8, 9585 g Tricine

0, 5 g SDS

Fill up to 50 ml w/ H<sub>2</sub>O

#### **10X Anode buffer (100 mM Tris-HCl, pH 8.9)**

60, 57 g Tris

9, 38 ml 37% HCl (0,225M)

Fill up to 500 ml w/ H<sub>2</sub>O

**Table 10 - Tris-Tricine SDS-PAGE recipes**

	<b>Stacking And Separating Gels</b>			Total
	4% gel (stacking)	10% gel (spacer)	16% gel (separating)	
AB-6 (ml)	1	6	10	17
Gel Buffer (3X) (ml)	3	10	10	23
Glycerol (g)	-	3	3	6
Add water to final volume (ml)	12	30	30	72
Polymerase by adding:				
APS (10%) $\mu$ l	90	150	100	340
TEMED $\mu$ l	9	15	10	34

**AB-6 (for optimal resolution of small proteins and peptides):** 46.5 g of acrylamide 3 g of bisacrylamide in 100 ml of water.

**3X Sample Buffer for Tricine SDS-PAGE (for small peptides):**

3% SDS (wt/vol), 6% mercaptoethanol (vol/vol), 30% glycerol (wt/vol), 0.05% Coomassie blue G-250, 150 mM Tris/HCl (pH 7.0)

## APPENDIX B

### SINGLE LETTER AMINO ACID CODES

G - Glycine (Gly)

P - Proline (Pro)

A - Alanine (Ala)

V - Valine (Val)

L - Leucine (Leu)

I - Isoleucine (Ile)

M - Methionine (Met)

C - Cysteine (Cys)

F - Phenylalanine (Phe)

Y - Tyrosine (Tyr)

W - Tryptophan (Trp)

H - Histidine (His)

K - Lysine (Lys)

R - Arginine (Arg)

Q - Glutamine (Gln)

N - Asparagine (Asn)

E - Glutamic Acid (Glu)

D - Aspartic Acid (Asp)

S - Serine (Ser)

T - Threonine (Thr)

## APPENDIX C

### PROTOCOL FOR SILVER STAINING

#### Step 1

1 hour or over night fixing at:

- 150 ml methanol
- 36 ml acetic acid
- 150  $\mu$ l 37% Formaldehyde
- completed to 300 ml with dH<sub>2</sub>O

#### Step 2

15 min washing in freshly prepared 50% ethanol

#### Step 3

1 min pre-treatment at:

0.02 g Na<sub>2</sub>S<sub>2</sub>O<sub>3</sub>.5H<sub>2</sub>O (Sodium thiosulfate)

100 ml dH<sub>2</sub>O

Solution should be mixed with a glass rod and 2 ml should be taken to another tube to be used in later steps

#### Step 4

Rinse with dH<sub>2</sub>O for 5 sec to remove excess of sensitizer



**Step 5**

Wait the gel for 20 min in impregnate solution. At this step silver ions saturate the gel and proteins, due to interactions with the negatively charged amino acids.

Impregnate solution:

- 0.2 g silver nitrate
- 100 ml dH<sub>2</sub>O
- 75 µl 37%Formaldehyde

**Step 6**

Rinse with dH<sub>2</sub>O for 20 sec two times

**Step 7**

Place the gel in developing solution for 2 minutes to reduce protein bound silver ions to metallic silver which leads to the development and visualization of protein bands. After a few minutes, some dH<sub>2</sub>O can be added to precede the reaction slowly.

**Step 8**

Rinse with dH<sub>2</sub>O for 2 min two times

**Step 9**

Place the gel to stop solution. Stop solution terminates silver ion reduction to avoid high background due to prolonged developing. Gel can be scanned or dried for long term storage.

Stop solution:

- 200 ml methanol
- 48 ml acetic acid
- completed to 400 ml with dH<sub>2</sub>O